


Article

CIM-Powered Multi-Hazard Simulation Framework Covering both Individual Buildings and Urban Areas

Xinzheng Lu ^{1,*}, Donglian Gu ², Zhen Xu ³, Chen Xiong ⁴ and Yuan Tian ²

¹ Key Laboratory of Civil Engineering Safety and Durability of China Education Ministry, Department of Civil Engineering, Tsinghua University, Beijing 100084, China

² Beijing Engineering Research Center of Steel and Concrete Composite Structures, Tsinghua University, Beijing 100084, China; lvlivegd_l_thu@163.com (D.G.); abcttyy01@163.com (Y.T.)

³ School of Civil and Resource Engineering, University of Science and Technology Beijing, Beijing 100083, China; martin31567@163.com

⁴ Guangdong Provincial Key Laboratory of Durability for Marine Civil Engineering, Shenzhen University, Shenzhen 518060, China; xiongchen@szu.edu.cn

* Correspondence: luxz@tsinghua.edu.cn

Received: 2 May 2020; Accepted: 19 June 2020; Published: 21 June 2020



Abstract: To improve the ability to prepare for and adapt to potential hazards in a city, efforts are being invested in evaluating the performance of the built environment under multiple hazard conditions. An integrated physics-based multi-hazard simulation framework covering both individual buildings and urban areas can help improve analysis efficiency and is significant for urban planning and emergency management activities. Therefore, a city information model-powered multi-hazard simulation framework is proposed considering three types of hazards (i.e., earthquake, fire, and wind hazards). The proposed framework consists of three modules: (1) data transformation, (2) physics-based hazard analysis, and (3) high-fidelity visualization. Three advantages are highlighted: (1) the database with multi-scale models is capable of meeting the various demands of stakeholders, (2) hazard analyses are all based on physics-based models, leading to rational and scientific simulations, and (3) high-fidelity visualization can help non-professional users better understand the disaster scenario. A case study of the Tsinghua University campus is performed. The results indicate the proposed framework is a practical method for multi-hazard simulations of both individual buildings and urban areas and has great potential in helping stakeholders to assess and recognize the risks faced by important buildings or the whole city.

Keywords: multiple hazards; CIM; BIM; GIS; physics-based hazard analysis; high-fidelity visualization

1. Introduction

1.1. Multi-Hazard Simulation

Generally, buildings in a built environment may encounter more than one potential major hazard at any given time. For example, Osaka city in Japan is not only prone to a high earthquake risk owing to earth tectonics, but also typhoon and fire risks due to its offshore geographical location and large number of wooden houses. In recent years, the performance of the built environment when subjected to multiple hazards has attracted much attention. Furthermore, with regard to the hazard resistance of the built environment, it must be kept in mind that stakeholders may focus on objects of different scales. For example, for a city manager who is responsible for the decision making related to the risk assessment of the whole city, apart from the overall performance of the city under multiple hazards, the hazard resistance of some specific buildings (e.g., the office building of the government) is also

important owing to their special strategic value. Nowadays, with the continuous development of smart city technology, a multi-hazard simulation tool that can consider both individual buildings and urban areas is needed more than ever. The realization of such a multi-hazard simulation tool for a real region can definitely bring significant technological progress and efficiency improvement in many fields, especially in disaster prevention and risk assessment. However, to the authors' knowledge, studies related to a multi-hazard simulation method covering both individual buildings and urban areas are rarely found in previous research.

Motivated by the abovementioned significant demands, this study is going to propose a multi-hazard simulation framework covering both individual buildings and urban areas. The hazards encountered by a city include various types, e.g., earthquake, urban fire, wind hazard, flood, tsunami, etc. It should be noted that considering all types of hazards simultaneously is beyond the scope of this work. Conversely, earthquake, fire, and wind hazards, which are the three important threats to buildings in China [1–3], are considered in this study. Given the scalability of the simulation framework proposed in this study, the corresponding simulation modules for other hazards can be developed and added to the framework in future research. Furthermore, the realization of such an integrated simulation tool is undeniably an enormous research topic, involving many great challenges such as the data architecture of building information, the deduction algorithms of multiple hazards, the visualization methods of results, and the integration of all these data and algorithms. It is difficult for this work to solve all the above problems. Instead, this study will focus on the possible solutions to the problems of multi-hazard simulation and visualization methods.

1.2. Literature Review

Although a multi-hazard simulation framework considering both individual buildings and urban areas is rarely found in previous research, this topic can be divided into two sub-topics based on the scale of the object to be modeled, i.e., multi-hazard simulation for individual buildings and multi-hazard simulation for urban areas, and some achievements of the two sub-topics can be found in the existing literature.

1.2.1. Multi-Hazard Simulation for Individual Buildings

Many researchers have studied the simulation of earthquake, fire, or wind hazards for individual buildings. According to the state-of-the-art literature, the technology of single-hazard simulation for individual buildings is relatively mature [1–7]. However, when it comes to multi-hazard simulation, a new problem needs to be addressed—different hazard analyses demand different building data formats. Specifically, earthquake simulations require the finite element (FE) model of the structures; fire simulations require information on the entire building, including structural and non-structural components as well as some indoor equipment, such as sprinkler systems [8]. The simulation of a wind field around a specific building requires information only on the building exterior surfaces, because the objects inside the building have no interaction with the wind field outside in the condition that the fluid-structure interaction is not considered. Therefore, without a unified data format for multi-hazard simulation, a user has to build several models for the corresponding hazard analyses, which is time-consuming and labor-intensive. Furthermore, continuous changes occurring in both the internal and external conditions of buildings make it difficult to maintain the models for different hazard analyses. Thus, it is important to (1) unify the fundamental data format of individual buildings needed for multi-hazard simulation and (2) realize a convenient transformation from fundamental data into models for different hazard analyses in order to facilitate a dynamic update of building information and promote the efficiency of multi-hazard simulations.

1.2.2. Multi-Hazard Simulation for Urban Areas

Research on hazard simulation for urban areas was performed much later when compared to research on hazard simulation for individual buildings, yet some remarkable outcomes have been

achieved. Currently, one of the most famous multi-hazard simulation frameworks for urban areas is HAZUS, which was developed by the Federal Emergency Management Agency (FEMA) of the United States. HAZUS is a nationally applicable standardized methodology based on the geographic information system (GIS), containing the models for estimating the potential physical, economic, and social impacts of earthquakes, fires following earthquakes, floods, and hurricanes [9]. However, recent studies have offered more advanced solutions for different hazard analyses than the existing modules in HAZUS. Specifically, with regard to regional earthquake simulations, HAZUS uses the capacity spectrum method based on the single degree-of-freedom (SDOF) model [10]. In contrast, multiple degree-of-freedom (MDOF) models in conjunction with nonlinear time history analysis (THA) proposed in recent years [11,12] are more accurate owing to their rational consideration of the features of different buildings and ground motions. For regional fire simulations, a fire-spread model developed by Hamada in 1975 [13] was adopted by HAZUS, which is entirely empirical and unable to rationally consider the effects of weather conditions (e.g., ambient temperature) and the fire resistance of buildings with different structural types, unlike physics-based urban fire-spread models developed in recent years [14–17]. With respect to wind simulations for a region, wind loads on building surfaces specified in HAZUS are derived using a hybrid code/directional model that adopts code-specified loads in conjunction with the empirical directional model [18]. This approach does not consider the influence of adjacent buildings as well as the interaction between buildings and the terrain. In contrast, recent developments in computational fluid dynamics (CFD) [19] may provide a tool for remedying the abovementioned defects [20–26]. Owing to all the reasons cited above, it is necessary to introduce new physics-based methods into multi-hazard simulations for urban areas.

In addition to the drawbacks of hazard analysis models, the visualization of outcomes from HAZUS needs to be improved. Users of the multi-hazard simulation technology include not only professionals, but also non-professional people with a limited knowledge of hazards (e.g., decision makers). To help non-professional people better understand hazard scenarios, a high-fidelity visualization of hazard analysis results is desired to encourage the use of multi-hazard simulation technology.

Apart from HAZUS, the Interdependent Networked Community Resilience Modelling Environment (IN-CORE) [27] is also a well-known multi-hazard simulation tool. The National Institute of Standards and Technology (NIST) funded the multi-university five-year Center of Excellence for Risk-Based Community Resilience Planning (CoE) to develop this integrated tool, and now the first version of IN-CORE has been released. The impact of the earthquake and tsunami hazards on community resilience can be modeled through the existing version of IN-CORE, and the hurricane, coastal storm surge, and riverine flooding hazards will be included in the next version. However, compared with state-of-the-art modeling technologies, similar challenges also exist in this tool. As an instance, the capacity spectrum method used by HAZUS for regional earthquake simulations is also adopted by IN-CORE, indicating that the high-order modes of structures and the time-domain features of different ground motions cannot be rationally considered in IN-CORE. More details of IN-CORE can be found on its official website [27].

1.2.3. Summary of the Literature Review

As introduced above, the existing multi-hazard simulation technology for individual buildings or urban areas can be improved from several aspects. Specifically, in terms of individual buildings, the fundamental data format needed for multi-hazard simulation has to be unified to facilitate a dynamic update of building information and promote simulation efficiency. With regard to urban areas, compared with the empirical models in the existing multi-hazard simulation platforms, the physics-based models need to be utilized to realize highly rational and scientific simulations, and the visualization of outcomes from the existing platforms needs to be improved to help non-professional people better understand hazard scenarios. Table 1 summarizes the contributions of this study compared with the previous research.

Table 1. Comparisons between the present study and previous research.

	Previous Research	Present Study
Multi-hazard simulation framework covering both individual buildings and urban areas	Studies related to this topic are rarely found in previous research.	To propose such a framework based on a unified data format containing the building information of both individual buildings and urban areas.
Multi-hazard simulation for individual buildings	Different hazard analyses demand different building data formats, resulting in a user having to spend much time and labor on building several models for different hazard analyses [1–7].	To realize multi-hazard simulation for individual buildings based on a unified database.
Multi-hazard simulation for urban areas	(1) The existing platforms adopt empirical or semi-empirical models for several hazards, which lack adaptability given their dependence on historical disaster data [9,10,18,27]. (2) The visualization of outcomes from the existing platforms needs to be improved [9,27].	To propose a physics-based simulation framework with high-fidelity visualization of analysis results.

1.3. Overview of this Study

The motivation of this work is to propose a novel multi-hazard simulation framework for both individual buildings and urban areas to help the stakeholders like city managers to assess and recognize the risks faced by important buildings or the whole city more scientifically and efficiently. The proposed multi-hazard simulation framework considers three types of hazards (i.e., earthquake, fire, and wind hazards) and is composed of three modules—(1) transformation from a unified database into corresponding physics-based models for different hazard analyses, (2) physics-based hazard analysis for both individual buildings and urban areas, and (3) high-fidelity visualization. It should be noted that the proposed multi-hazard simulation framework utilizing several simulation tools does not equal a completely integrated simulation platform, as developing such a powerful tool is undeniably an enormous research topic and beyond the scope of this study. Even so, the proposed framework can provide a reference for research on data transformation technology, the physics-based building modelling method, as well as the high-fidelity visualization method. Moreover, this work will help to close the gap between the existing research and a truly highly integrated tool, leading to an integrated platform in the future. It is also worth pointing out that the proposed simulation framework is applicable to buildings in China. However, given that the physics-based building models adopted in the framework do not rely on the historical hazard data of the target area, the proposed framework can still be used for other areas (e.g., Japan) if the corresponding modelling methods for regional buildings (introduced in Section 3.2.) are modified based on the building data of the target area.

In the following sections, the overall workflow of the proposed multi-hazard simulation framework is firstly introduced. Subsequently, the methodologies of the three modules for different hazard analyses (i.e., earthquake, fire, and wind simulations) are discussed. A case study of the entire Tsinghua University campus was performed by implementing the proposed framework.

2. The Proposed Multi-Hazard Simulation Framework

2.1. City Information Model

To address the problems mentioned above, it is necessary to unify a fundamental data format required by multi-hazard simulations for both individual buildings and urban areas. It is well known that GIS [28] and the building information model (BIM) [29] are two famous means of managing building data. GIS is an efficient platform for storing urban data. Users can add and store various kinds of information on urban areas in GIS platforms, such as terrain, building location, and building

occupancy [28]. However, when it comes to multi-hazard simulation for individual buildings, most GIS models cannot provide sufficient detailed information. Specifically, the building attributes expressed only by GIS are not rich enough to represent the detailed information of each component and equipment in a target building [30]. In contrast, BIM is a good choice for the high-fidelity expression of individual buildings. Powered by useful and abundant libraries in existing BIM programs for components, users can easily construct high-fidelity information models of individual buildings [8]. But BIM is not suitable for the data storage of a large number of buildings in urban areas, as creating refined BIM models for an urban area comprising hundreds of buildings is extremely time-consuming.

Owing to the above drawbacks of BIM and GIS, a new data management method covering both individual buildings and urban areas is needed to realize multi-hazard simulation based on a unified database. A city information model (CIM), which can be defined as the integration of GIS and BIM (see Figure 1), has been proposed and developed rapidly in recent years [30]. As it is armed with both the convenience of GIS in representing the spatial data of urban areas and the richness of BIM in expressing component information of individual buildings, CIM is considered a powerful tool for multi-hazard simulation of both individual buildings and urban areas, and is thus adopted as the fundamental data format in this study. According to the state-of-the-art literature, the applications of CIM primarily focused on building energy management [31,32], a smart city system [33,34], and a 3D heritage city model [35]. By contrast, little of the research considers utilizing CIM for the hazard simulation of buildings or regions. This work will fill a gap in this domain.

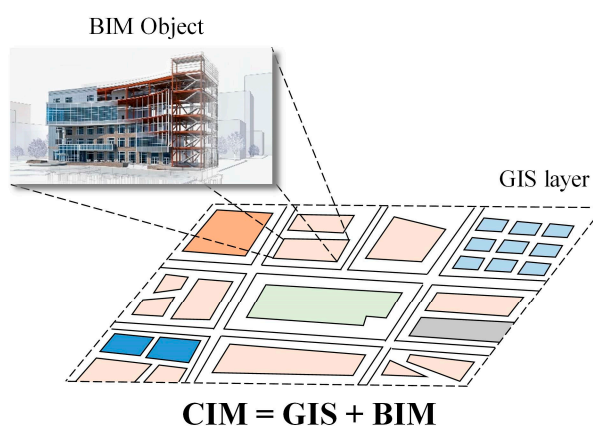


Figure 1. Concept of CIM.

Some remarkable progress has been achieved in the integration of BIM and GIS. According to the state-of-the-art literature, there are two main methods for integrating BIM and GIS [36–43]. The first method is based on the well-established BIM and GIS software, which adopts building information modelling to express details of the buildings and realizes 3D visualization on the GIS platform [36,37,40,42]. In contrast, in the second method, a unified expression format is designed to integrate BIM and GIS models, which is usually based on the Industry Foundation Classes (IFC) and CityGML [38,39,41,43]. The first method has the advantage of a convenient software interface, which is generally easy for users to utilize CIM tools for some typical applications, while the second one focuses on the design of the unified data architecture of CIM, which does not rely on any commercial modeling tools. In other words, the first method is to directly use an existing platform, while the second one is to redesign a new data architecture of CIM. Note that the main focus of this work is on the use of CIM for multi-hazard simulations covering both individual buildings and urban areas, instead of studying the integration method of BIM and GIS. Hence, the first method mentioned above was adopted in this study to realize the construction of CIM data, owing to the fact that its convenient software interface can be directly utilized without developing a new data architecture. Specifically, Revit [44] was adopted as the BIM tool, while SuperMap GIS 9D [45] was used as the GIS tool and CIM

visualization platform. Multi-hazard simulations covering both individual buildings and urban areas were based on the CIM data stored in SuperMap GIS 9D software.

2.2. Simulation Framework

The proposed multi-hazard simulation framework is illustrated in Figure 2. In the framework, Module 1 corresponds to data transformation, Module 2 corresponds to physics-based multi-hazard analysis, and Module 3 represents high-fidelity visualization. Detailed explanations of the modules are presented below.

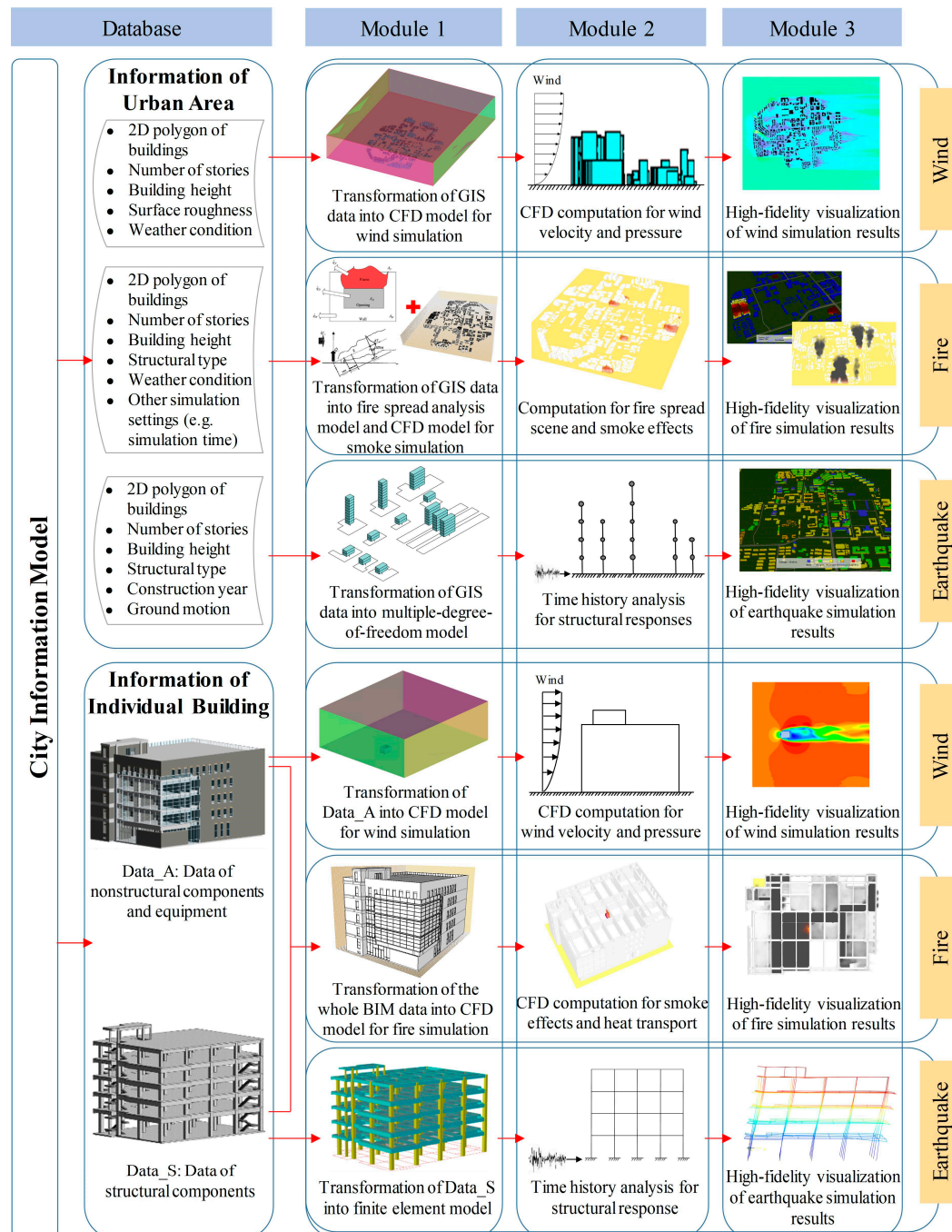


Figure 2. The proposed multi-hazard simulation framework for both individual buildings and urban areas.

2.2.1. Multi-Hazard Simulation for Individual Buildings

With regard to the individual building case in the proposed framework, the data needed for multi-hazard simulation of individual buildings taking earthquake, fire, and wind hazards into consideration is unified as BIM data stored in the CIM. With respect to different hazards, the framework realizes efficient and convenient information extraction from CIM data so that users are not required to build several models for different hazard analyses. Furthermore, the unified fundamental data format will facilitate dynamic updates of the building information. Even though some changes may occur in the target building, users can easily update multi-hazard simulation results based on the modified CIM data.

In terms of earthquake hazards, information on the structural components of a specific building stored in the BIM data was used for FE analysis in Module 1 of the proposed framework, after which nonlinear THA was performed in Module 2, and the engineering demand parameters (EDPs; e.g., deformation) derived from THA were visualized in Module 3. With respect to fire hazards, because both structural and non-structural components affect fire simulation, information on the structural and non-structural components as well as on the equipment stored in the BIM data was transformed into the CFD model for fire simulation in Module 1. Subsequently, CFD simulation was implemented in Module 2, and the simulation results (e.g., smoke and temperature) were visualized in Module 3. For wind hazards, note that only the exterior surfaces of a building exert an impact on the wind field around the building, because the objects inside the building have no interaction with the wind field outside in the condition that the fluid-structure interaction is not considered. To avoid difficulties in the mesh generation of the CFD model due to complicated indoor components, Module 1 firstly extracted data corresponding to the exterior building surfaces for CFD simulation. Subsequently, CFD simulations were performed in Module 2, and the outcomes (e.g., pressure and speed) were visualized in Module 3.

2.2.2. Multi-Hazard Simulation for Urban Areas

With regard to urban areas in the proposed multi-hazard simulation framework, the data needed for earthquake, fire, and wind simulations was unified as GIS data, which could be extracted from the CIM. Two types of data are generally stored in the GIS platform—(1) building data (e.g., building height, number of stories, building geometry, building occupancy, structural type, and construction year) and (2) simulation settings (e.g., ground motion and weather condition). With regard to an earthquake hazard, building data stored in GIS was firstly transformed into MDOF models. Subsequently, city-scale nonlinear THA was performed in Module 2 according to the ground motion information stored in GIS data. EDPs were visualized using a high-fidelity visualization method in Module 3. For fire hazards, a physics-based fire-spread model and CFD-based smoke simulation model were derived from the building data in Module 1. Module 2 implemented the fire spread and smoke simulations. Module 3 visualized the fire-spread scenario and smoke effect using different visualization methods. With respect to wind hazards, the CFD model for wind simulation was derived from the building data stored in GIS in Module 1, and CFD computations were implemented in Module 2. The simulation results were finally visualized in Module 3.

Furthermore, it should be noted that hazard analysis models for urban areas in the proposed framework are all physics-based models. Specifically, in terms of regional earthquake simulations, the MDOF models in conjunction with nonlinear THA [12] were utilized in the proposed framework, which leads to more accurate simulation results due to the rational consideration of the features of different buildings and ground motions. With regard to regional fire simulations, a physics-based fire-spread model proposed by Zhao [17] was used in the proposed framework. In Zhao's model, fire development in an individual building (i.e., ignition, flashover, full-development, collapse, and extinguishment) was simplified by defining the temperature and heat-release rate of the burning building versus time, while fire spread between buildings was realized through two main mechanisms, namely thermal radiation and thermal plume. Consequently, the fire-spread model took the effects of

wind and fire resistance of different buildings into account. Meanwhile, the smoke scenario was also based on the predicted fire-spread scenario and CFD simulations [46]. With respect to wind simulations for a region, CFD simulations used in the proposed framework are capable of considering the influence of adjacent buildings as well as the interaction between different buildings and the terrain [47–49].

3. Methodology

Detailed explanations of the underlying methodologies for each hazard analysis are presented below. The following two sections introduce the methodologies used for individual building and urban area cases, respectively.

3.1. Individual Building Case

3.1.1. Earthquake Simulation

BIM application in the structural domain is an important topic of research. There are numerous studies on the automatic generation of structural analysis models based on BIM [50–53]. Therefore, related topics are not discussed in detail herein. General purpose MSC.Marc software [54] was selected for FE analysis, and a program named IFC2MARC developed by Zeng et al. [55] was employed for direct data transformation from BIM to FE model. The data transformation workflow is shown in Figure 3, and the details of the program can be found in Zeng et al. [55]. Furthermore, the social and economic impact (i.e., casualties, repair time, and economic losses) can also be predicted using EDPs from nonlinear THA and seismic performance assessment methodology (e.g., FEMA P-58) [10,56].

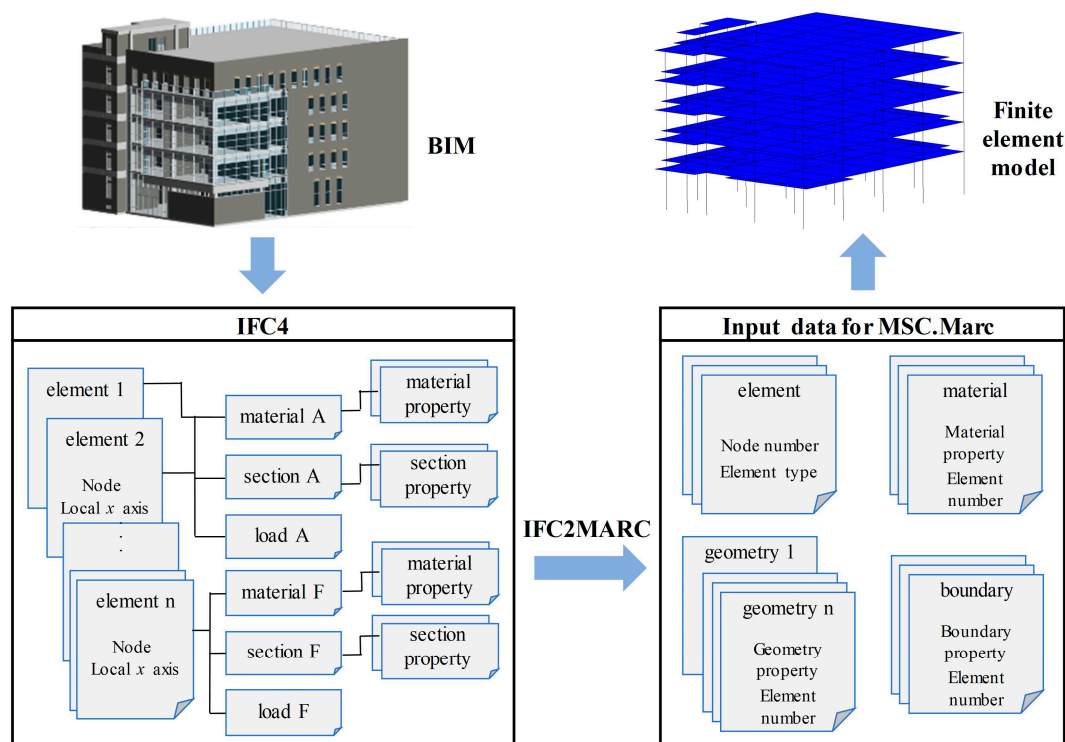


Figure 3. Transformation from BIM data into the FE model.

3.1.2. Fire Simulation

In this study, Fire Dynamic Simulator (FDS) [57], an internationally well-accepted fire simulation program developed by NIST, was adopted for fire simulation. The FDS model was established based on BIM using the model transformation method proposed by Xu et al. [8]. Specifically, geometry information of the components in BIM was exported to the FDS model using a pre-processing program,

Pyrosim [58]; meanwhile, the material information of components in the BIM was transformed to the FDS model using the program FDS_BUILD built by Xu et al. [8]. The whole process of data transformation is shown in Figure 4.

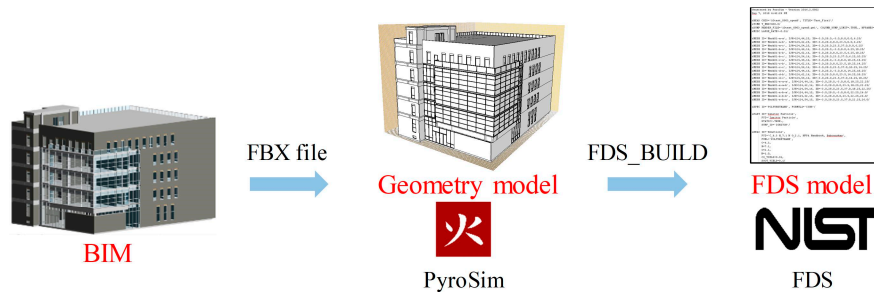


Figure 4. Transformation from BIM data into the FDS model.

Indoor fire simulation can be performed in FDS after the FDS model is constructed. Smokeview [57], a post-processing software for FDS, provides a tool for visualizing simulation results with high fidelity. Simulation results, such as soot density and temperature, can be further used to predict the evacuation behavior of people in a fire hazard situation [59].

3.1.3. Wind Simulation

ANSYS Fluent, which is a widely used CFD software [60], was adopted for wind simulation in this study. Note that only the exterior surfaces of a specific building affect the wind environment around it. Based on Dynamo [61], an open-source visual programming tool and an official plug-in for Revit, a pre-processing program named BIM_ES was developed herein to extract the data of exterior surfaces from BIM. The workflow of BIM_ES is illustrated in Figure 5. Taking the process of extracting the exterior surfaces data of walls as an example, a function named ‘Select Model Elements’ was firstly used to collect the exterior components that should be processed, from which the ‘List.RemoveIfNot’ function was then called to filter out the components belonging to ‘wall’ type. Subsequently, three functions (‘Element.Geometry’, ‘PolySurface.BySolid’, and ‘PolySurface.Surfaces’) were invoked to obtain geometry information of all the exterior walls, following which exterior surface data of all the exterior walls was filtered through five functions named ‘Surface.FilterByOrientation’, ‘Surface.NormalAtParameter’, ‘Wall.ExteriorDirection’, ‘Vector.IsAlmostEqualTo’, and ‘List.FilterByBoolMask’. To further consider the thickness of the walls, the ‘Surface.PointAtParameter’ function was utilized to obtain points from each surface obtained from the former step. Synchronously, all the exterior wall components were combined through a function named ‘Solid.ByUnion’. The exact surfaces considering the thickness of the walls can be obtained through four functions (‘Geometry.Explode’, ‘Geometry.DoesInterest’, ‘List.AllIndicesOf’, and ‘List.GetItemAtIndex’). Finally, all the exterior surfaces were exported to a stereolithography (STL) file by two functions ‘Mesh.ByGeometry’ and ‘Mesh.ExportMeshes’ for subsequent CFD simulation.

The data transformation method for the wind simulation of individual buildings is shown in Figure 6. The STL file was generated using the BIM_ES program. The CFD mesh can be generated based on the STL file using some well-established pre-processing software (e.g., ICM CFD [60]). CFD simulation was conducted based on the meshed model and the corresponding simulation settings (e.g., boundary condition, turbulence model, equation solution method, and convergence criteria). Note that the simulation settings must meet the requirements specified in the latest best practice guidelines, such as COST 732 [62] and AIJ [63]. There are three turbulence models in CFD, viz. direct numerical simulation (DNS), large eddy simulation (LES), and Reynolds-averaged Navier-Stokes equations (RANS). Users can choose one of these methods to perform CFD simulations according to the simulation demand. The simulation results were visualized by a third party software named Tecplot 360 [64].

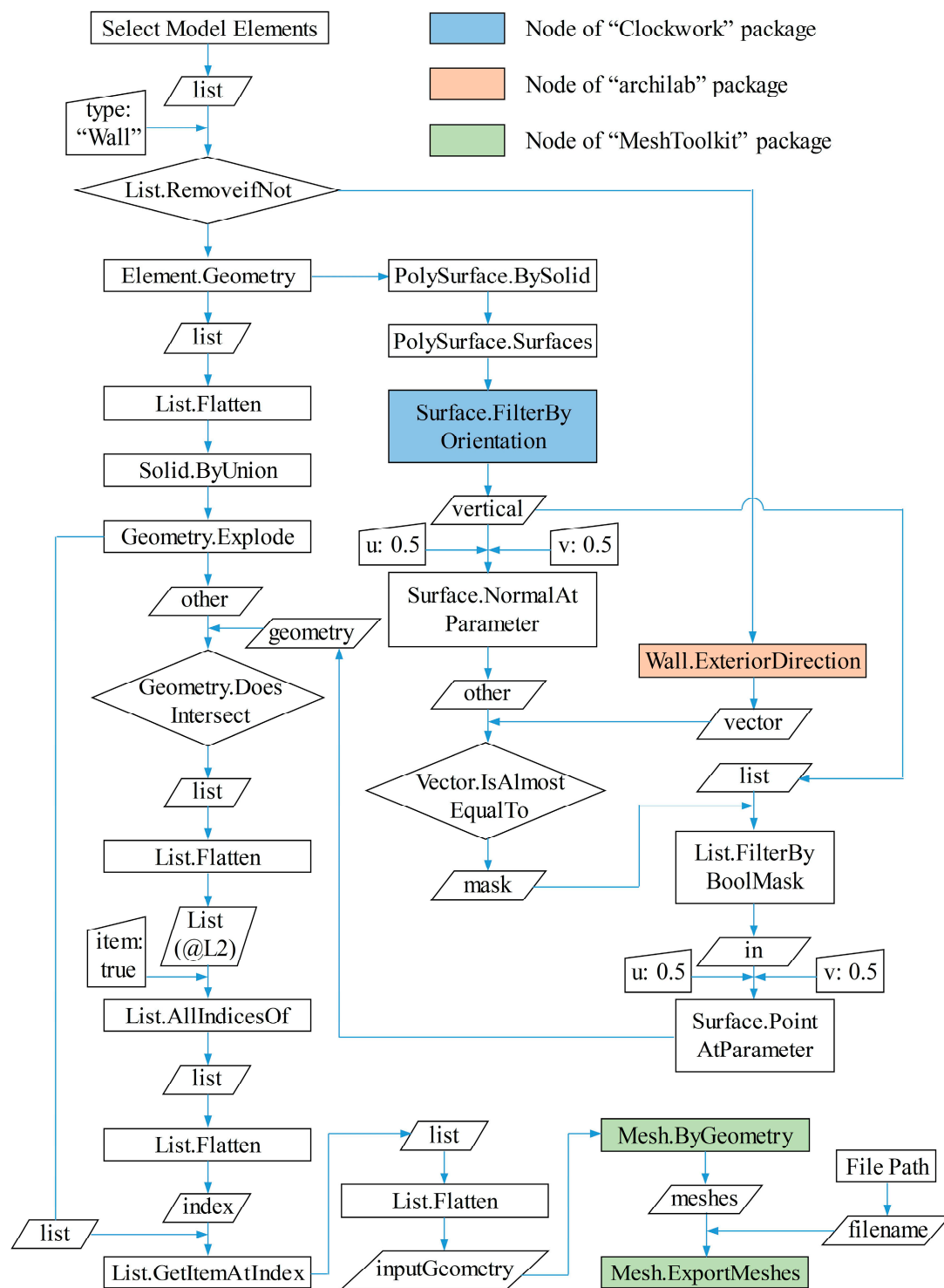


Figure 5. The workflow of BIM_ES program.

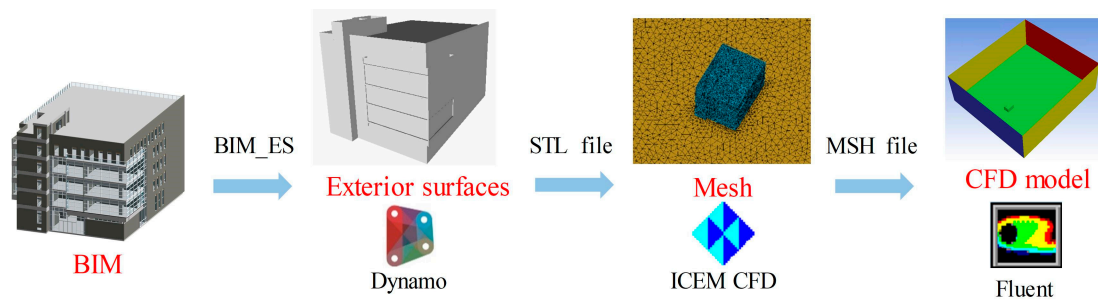


Figure 6. Transformation from BIM data into the CFD model.

3.2. Urban Area Case

In the urban area case, GIS data was firstly extracted from CIM for multi-hazard simulation in the proposed framework. Note that the GIS data should be checked to avoid topological errors of building polygons.

3.2.1. Earthquake Simulation

City-scale nonlinear THA proposed by Lu and Guan [12] was adopted in this study. Lu and Guan [12] verified the reliability of this method by comparing the predicted values with actual damage due to some real earthquakes. Specifically, the MDOF shear model was used for multi-story buildings while the MDOF flexural-shear model was used for tall buildings (Figure 7). The backbone curve of the springs connecting different stories adopts the trilinear model recommended by HAZUS (Figure 8a). The hysteresis behavior was simulated using a pinching model with only one parameter (Figure 8b). Based on the GIS database, all the parameters of the MDOF models could be automatically determined from the basic building information (i.e., number of stories, height, year built, structural type, floor area, and occupancy) following the modelling approach proposed by Lu and Guan [12].

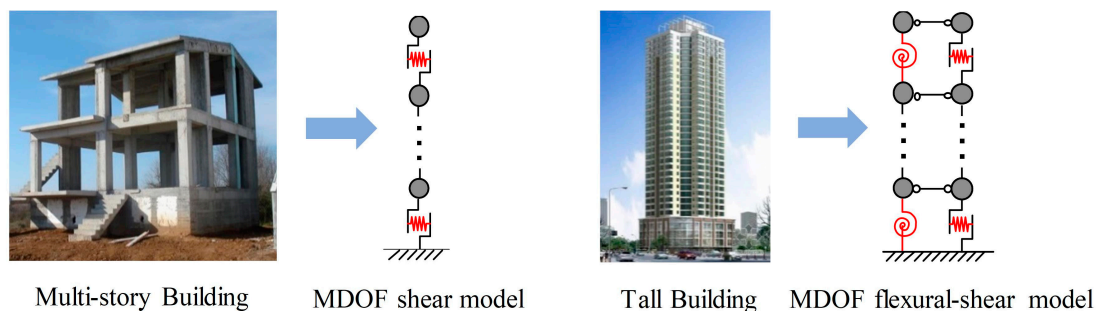


Figure 7. MDOF shear model for multi-story buildings and MDOF flexural-shear model for tall buildings.

Based on OpenSceneGraph (OSG) [65], an open source high-performance 3D graphics toolkit, the EDPs of the MDOF models were mapped into the corresponding vertices of the polygons of each building [66,67] in order to visualize the shaking of the whole urban area during an earthquake at high fidelity. In addition to building objects, other urban objects, such as terrain, roads, and vegetation, can also be visualized in the urban scene to improve the reality of visualization [66]. Furthermore, detailed inter-story drifts and floor acceleration generated by this method provide a much more accurate regional loss estimation according to the fragility function and consequence function of the FEMA P-58 report [68], which are important in determining the disaster prevention strategy for a city.

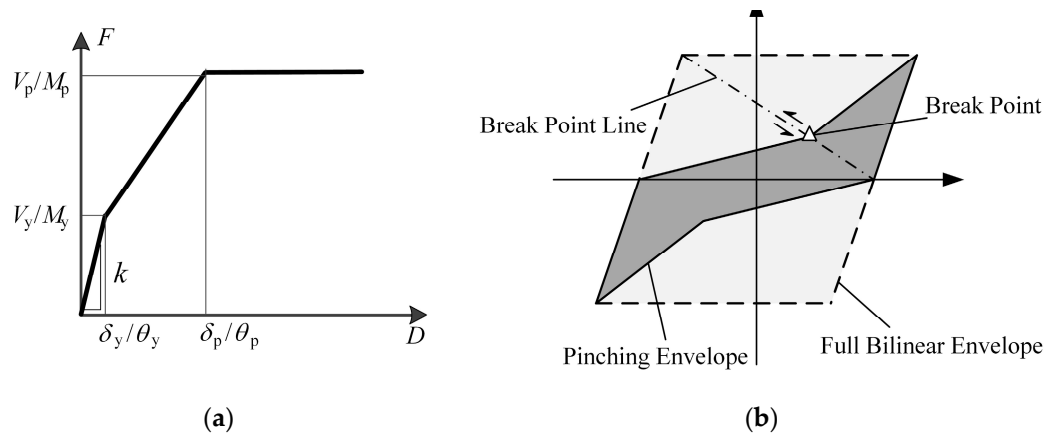


Figure 8. (a) Backbone curve and (b) pinching model of MDOF models.

3.2.2. Fire Simulation

A physics-based fire-spread model and visualization method for urban fire proposed by Zhao [17] are adopted in this study. Specifically, fire development in an individual building was simplified by defining the temperature and heat-release rate of the burning building versus time, while the simulation of fire spread between buildings was realized by considering thermal radiation and thermal plume mechanisms. Such a fire-spread model is capable of taking the effect of weather conditions (i.e., wind speed, wind direction, ambient temperature, humidity, and rain) and fire resistance of different buildings into account. The fire-spread model was validated by comparing the simulation with a real fire spread following the 1995 Kobe earthquake [17]. In terms of visualization, the OSG platform was utilized to present the process of fire spread among buildings and Smokeview software was used to visualize the smoke effect derived from the simulation performed in FDS [46].

The process of regional fire simulation was as follows. The building data (i.e., 2D polygon of buildings and structural type) and the simulation setting data (i.e., initial ignited building, weather condition, and simulation time) were extracted from the GIS data to perform fire-spread simulation, from which a list of fire-spread results (i.e., ignition time, burning duration, burned area) were obtained. Subsequently, building data (i.e., 2D polygon of buildings, building height, and number of stories) in conjunction with fire-spread results were imported into the OSG platform to visualize the fire-spread scene with high fidelity. Later, the 3D model of the specific urban area constructed in the OSG platform was exported to an OBJ file and then imported into FDS through PyroSim. The geometry of the urban area was defined by the '&OBST' keyword in FDS. Synchronously, the ignition time and burning duration of each ignited building were defined in FDS by the '&DEVC' and '&SURF' keywords, respectively, according to the fire-spread results. Other simulation settings, such as wind and simulation time, were also supplemented to the FDS model file. Finally, the FDS model file was submitted as a computational job and the simulation results were visualized in Smokeview. The whole workflow is illustrated in Figure 9.

3.2.3. Wind Simulation

Similar to the individual building case, ICEM CFD software was adopted for mesh generation, and ANSYS Fluent was used to perform CFD computation for wind simulations. To realize data exchange from GIS to ICEM CFD, a script was generated herein using ANSYS Mechanical APDL (MAPDL) [69], which can conveniently construct a 3D model of an urban area. For example, to establish a building model, whose bottom is a polygon with four vertices $((0, 0, 0), (0, 1, 0), (1, 1, 0), \text{ and } (1, 0, 0))$ and the height is 1.0, two APDL commands are needed: 'FLST, 2, 5, 8\n FITEM, 2, 0, 0, 0\n FITEM, 2, 0, 1, 0\n FITEM, 2, 1, 1, 0\n FITEM, 2, 1, 0, 0\n FITEM, 2, 0, 0, 0\n PRI2, P51X, 0, 0' and 'FLST, 2, 1, 5, ORDE, 1\n FITEM, 2, 1\n VEXT, P51X,,,0,0,1,,,,'. The former is used to construct the bottom polygon, and the second command stretches the polygon in the direction of height.

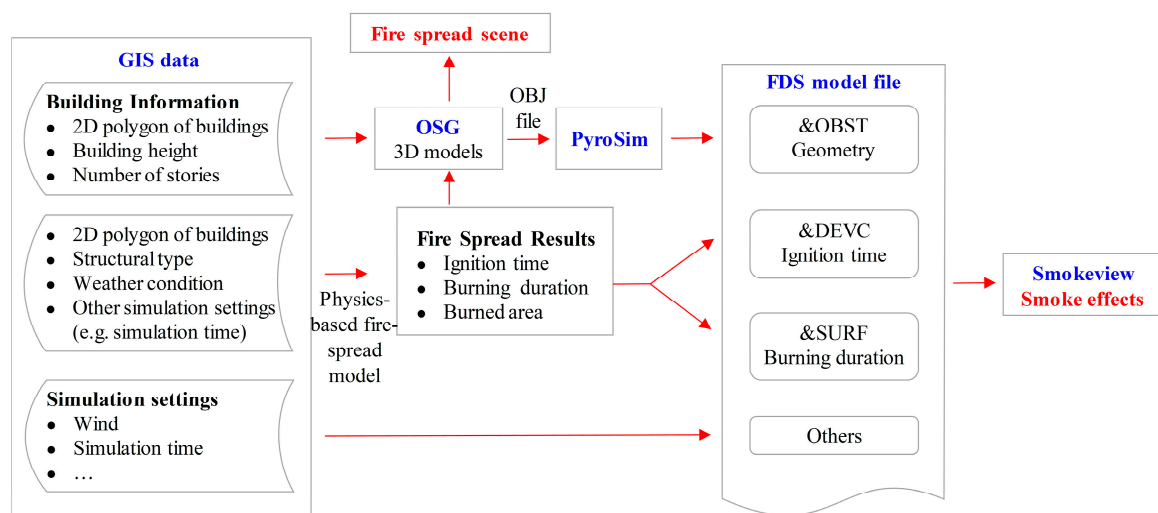


Figure 9. Data transformation of regional fire simulation.

As shown in Figure 10, the workflow of transformation from GIS data into the CFD model includes three steps. Firstly, a pre-processing program named GISStoAPDL was developed to transform GIS data into the 3D model of the specific urban area in MAPDL. Subsequently, the 3D model was exported to an initial graphics exchange specification (IGES) file and then imported into ICEM CFD for mesh generation. The computation and visualization procedures were the same as those used for the individual building case. The accuracy of the generated CFD model was sufficient to support decision making for urban planning, emergency management, and insurance [70].

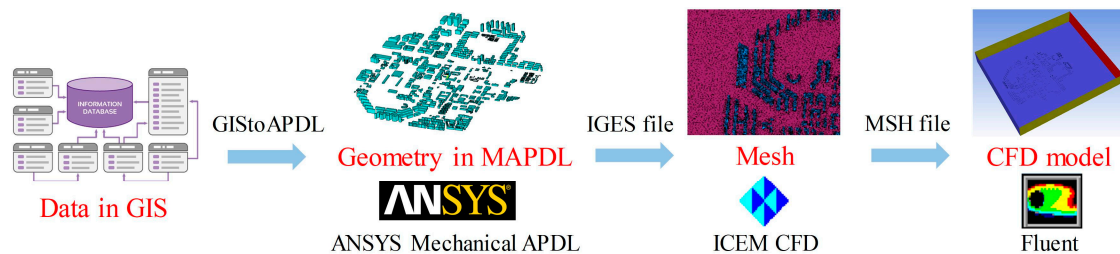


Figure 10. Transformation from GIS data into the CFD model.

4. Case Study

The Tsinghua University campus was selected as the case study to demonstrate the workflow of the proposed multi-hazard simulation framework. Apart from the overall performance of the campus under multiple hazards (i.e., earthquake, fire, and wind hazards), the hazard resistance of specific buildings is also important to administrators owing to their strategic value. Thus, a multi-hazard simulation covering the entire campus as well as some specific buildings was implemented to help administrators determine the appropriate disaster prevention and mitigation strategy.

4.1. Study Area

The Tsinghua University campus is located in the northwest of Beijing, China. The dimensions of the campus in the east-west and south-north directions are approximately 1.9 and 2.3 km, respectively. The occupancy and number of stories in each building are presented in Figure 11. More than half of the buildings are residential buildings and 78% of the buildings include less than five stories.

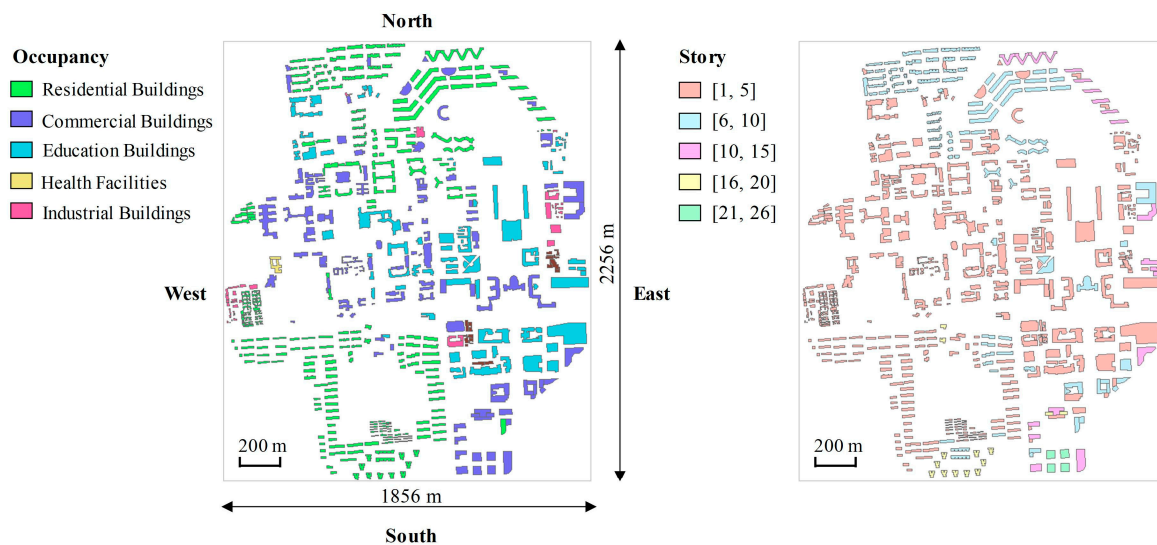


Figure 11. Buildings in the Tsinghua University campus.

The CIM of the entire campus constructed in this work consists of GIS data of 619 buildings in total and the BIM data of several important buildings. From the BIM data, an office building with four stories was selected to demonstrate multi-hazard simulation for individual buildings. The office building with a height of 17.5 m is located in the center of the campus, as shown in Figure 12a. It is a reinforced concrete (RC) frame structure and it was built in the year 1995. The detailed BIM of the office building is shown in Figure 12b.

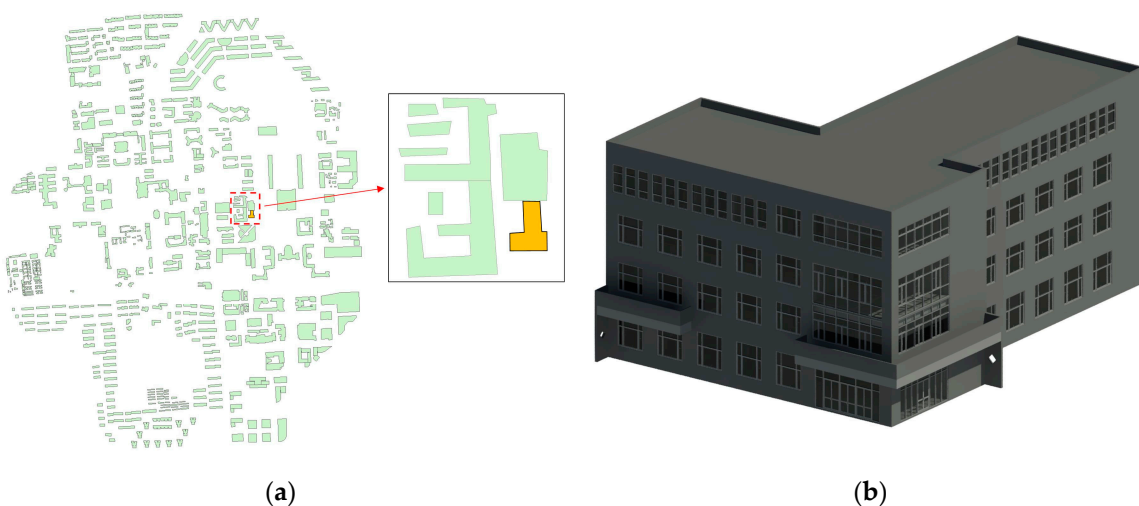


Figure 12. (a) Location and (b) BIM of the four-story office building.

4.2. Multi-Hazard Simulation of the Entire Campus

4.2.1. Earthquake Simulation

The horizontal component of El-Centro ground motion with a peak ground acceleration (PGA) of 0.40 g (corresponding to the maximum considered earthquake (MCE) hazard level with a return period of 2475 years, according to the Chinese Code for Seismic Design of Buildings [71]), along the south-north direction of the campus was adopted as the input for earthquake simulation. A city-scale nonlinear THA was performed. Subsequently, the predicted deformation of 619 buildings was visualized on the OSG platform, as shown in Figure 13. Furthermore, the detailed inter-story drifts and floor accelerations

generated by this simulation can be used to determine the damage state of each building [72]. As shown in Figure 14, unreinforced masonry structures were the most seriously damaged structures during the earthquake, followed by reinforced masonry structures and RC frame structures. RC frame-shear wall structures experienced the least damage. Therefore, strengthening unreinforced masonry structures is the key strategy to be employed for earthquake disaster prevention in the campus.

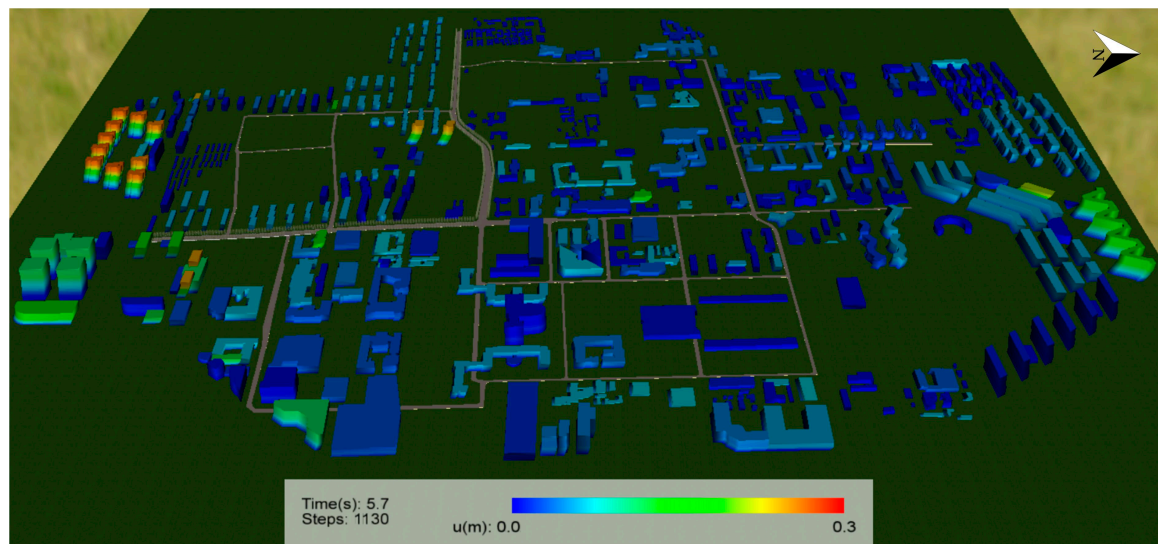


Figure 13. Deformation results of the buildings in the Tsinghua campus.

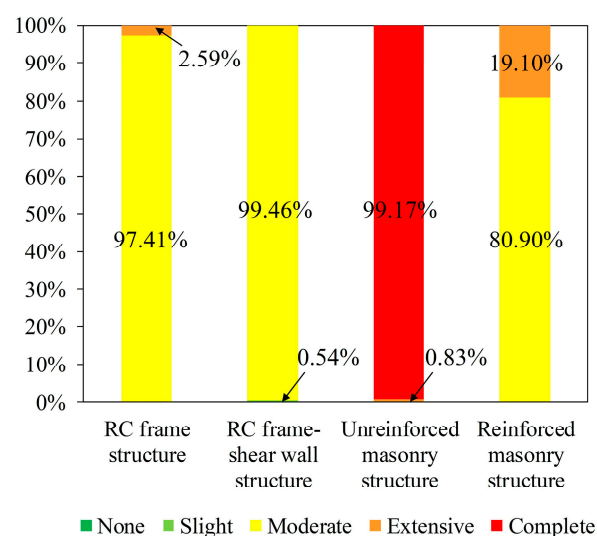


Figure 14. Predicted seismic damage states.

4.2.2. Fire Simulation

For fire simulation, six buildings of different occupancies were selected as the initial ignited buildings. The locations of these ignited buildings are identified in Figure 15. The reason for choosing these buildings as the initial ignited buildings is that they are located in different parts of the campus, so that the regional fire simulation can help administrators evaluate the risks of fire spread in different areas of the campus.

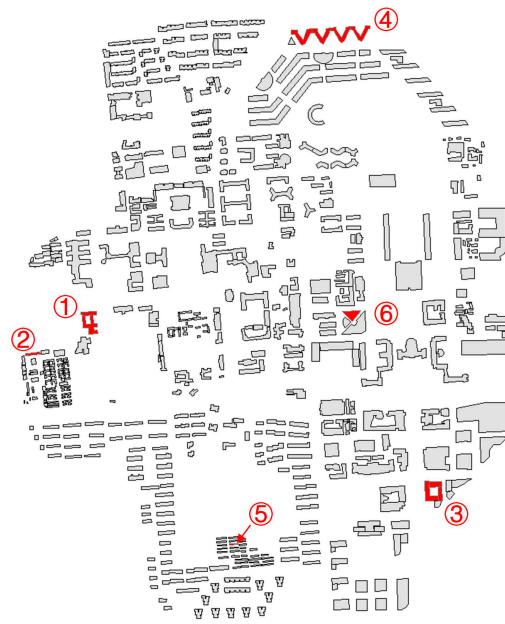


Figure 15. Locations of the ignited buildings.

A west wind condition (wind speed = 12 m/s), lowest ambient temperature of 6 °C, and highest ambient temperature of 16 °C were set for implementing regional fire simulation. The fire-spread scene was finally visualized in OSG (Figure 16). Even though the wind speed reached 12 m/s, fire spread mainly occurred around the office buildings located in the southeast of the campus; in addition, there was no fire spread in other areas owing to a rational fire separation between buildings. Figure 17 indicates that the fire situation stabilized after approximately four hours. The smoke effect was then visualized in Smokeview (Figure 18), which can enhance the reality of the fire scene and provide a high-fidelity virtual reality scene for practical applications such as fire disaster training [59].

4.2.3. Wind Simulation

For wind simulation, as the Tsinghua campus is approximately 1856 m × 2256 m in size with a height of $H = 78$ m for the tallest building, a computational domain of 3104 m × 3621 m × 508 m was constructed, ensuring an upstream length of 4.5 H , downstream length of 13 H , height of 6.5 H , and distance of 8 H from the campus to the lateral boundaries, which is in agreement with the COST 732 [62] and AIJ [63] best practice guidelines. RANS was utilized owing to its fast computation rate and relatively reliable results. North wind with a return period of 50 years was selected as an example. At the inflow, the mean speed profile was constructed following the values specified in the Chinese Load Code for the Design of Building Structures [73], which is given by Equation (1). The lateral and top boundary conditions were defined as frictionless walls following the best practice guidelines [62,63], and the outlet boundary condition was defined as free outflow. The standard wall law was adopted for the ground and building walls.

$$U(z) = \begin{cases} 21.627, & z \leq 15 \text{ m} \\ 11.941z^{0.22}, & 15 \text{ m} < z < 450 \text{ m} \\ 45.786, & z \geq 450 \text{ m} \end{cases} \quad (1)$$

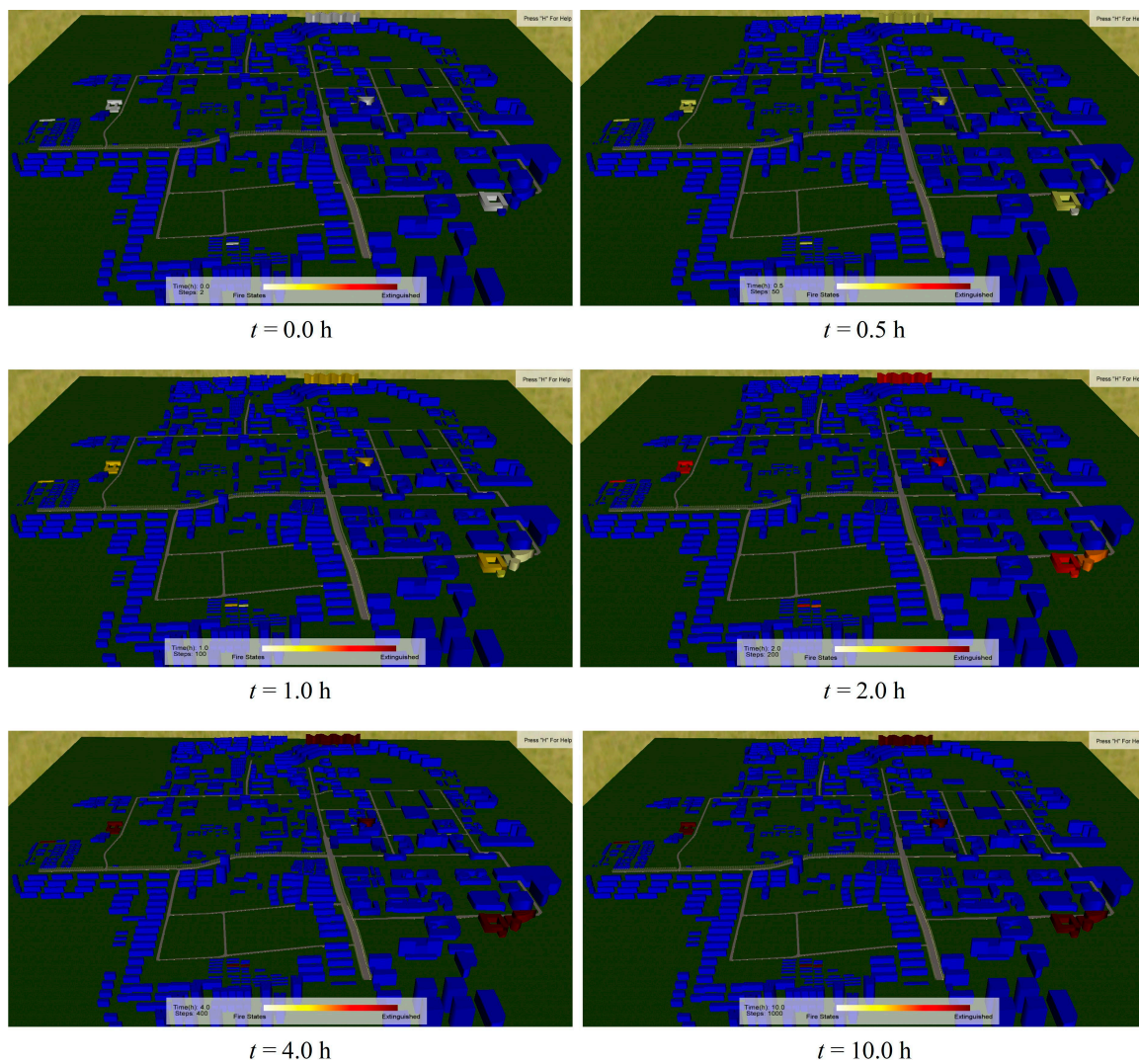


Figure 16. Time history of the fire-spread scene (wind speed = 12 m/s).

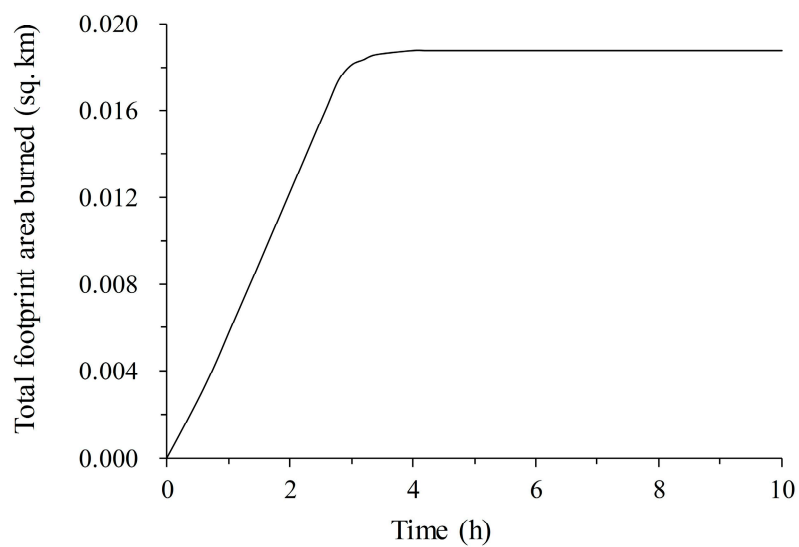


Figure 17. Total footprint area burned vs. time (wind speed = 12 m/s).

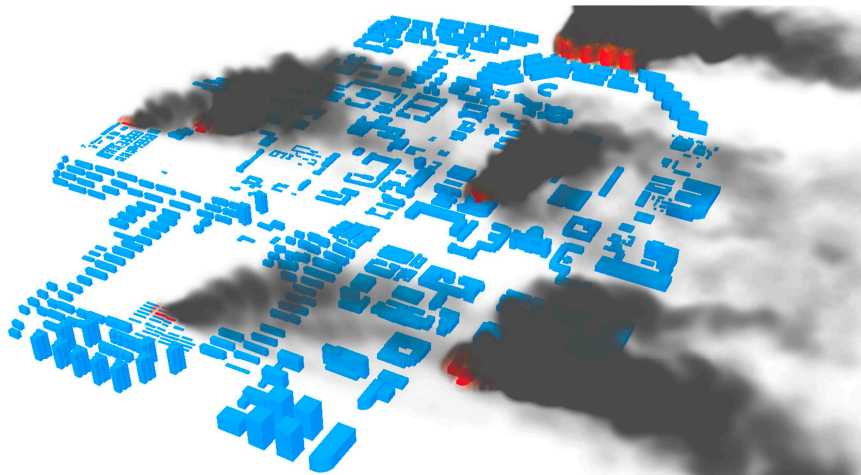


Figure 18. Smoke effects displayed in Smokeview (wind speed = 12 m/s).

Wind pressure on the exterior surfaces of buildings and wind speed at a height of 10 m are shown in Figures 19 and 20, respectively. The maximum positive and negative pressures on the exterior surfaces of the buildings were approximately 420 Pa and -1183 Pa, respectively. According to the fragility values of the non-structural components (e.g., roof covers, windows, and doors) obtained from HAZUS, the non-structural components of the buildings in the campus are free from severe damage in this wind scenario. In Figure 20, it can be seen that wind speed in most areas of the campus is much lower than the input speed due to the shading effect of multiple buildings.

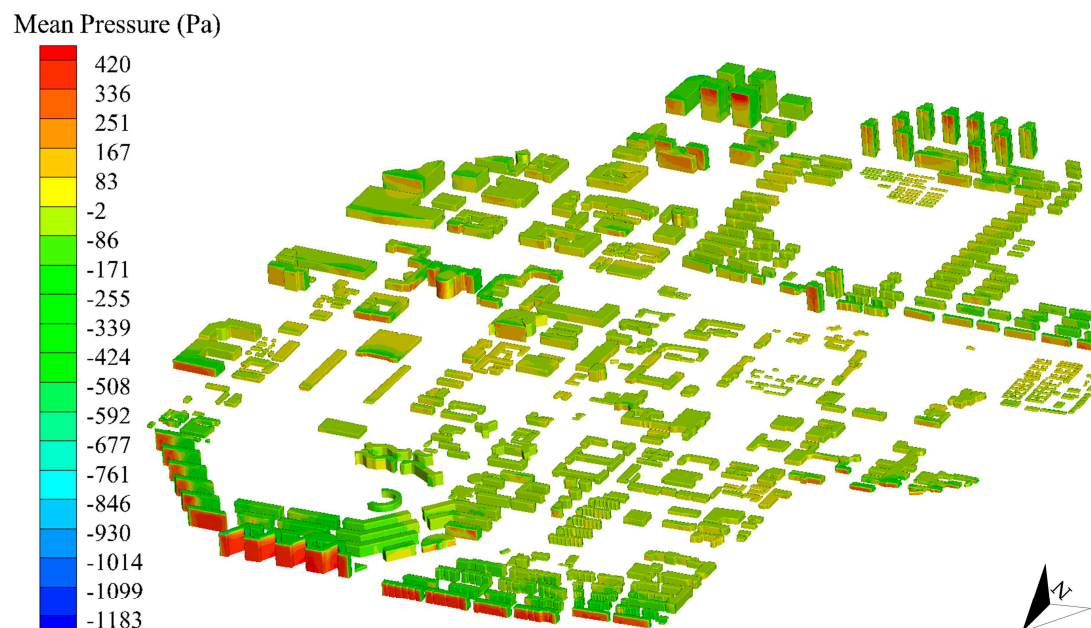


Figure 19. Wind pressure on the exterior surfaces of buildings in the Tsinghua campus.

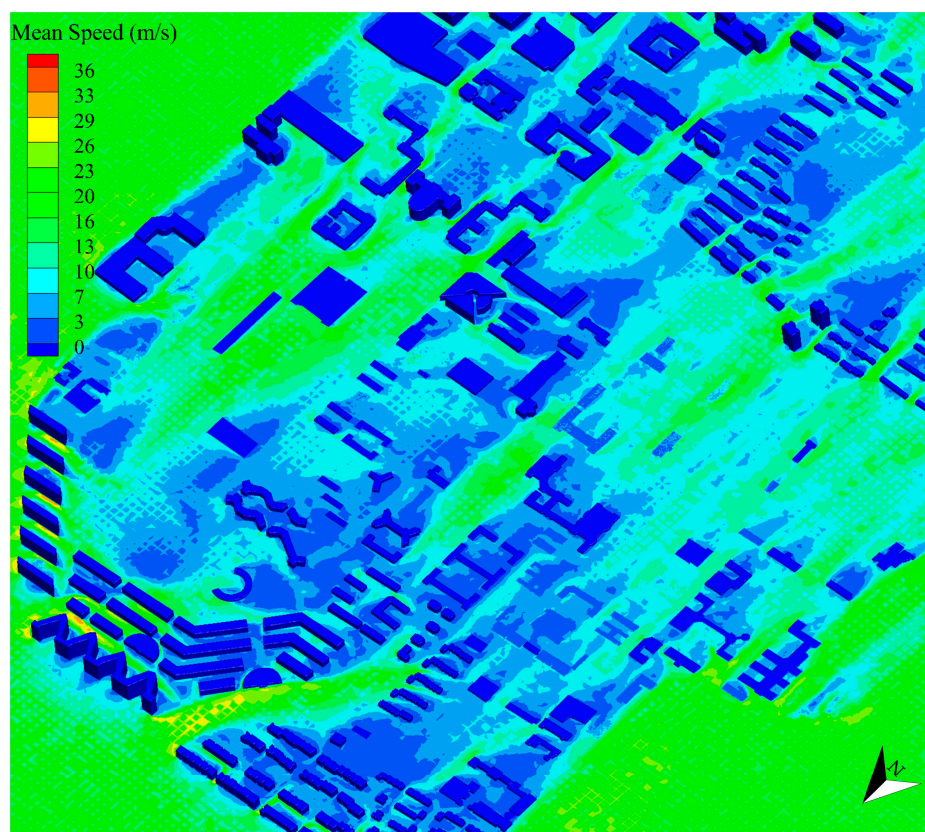


Figure 20. Wind speed at a height of 10 m.

Furthermore, the wind speed results can be used to evaluate the pedestrian wind comfort quality in the campus. In this study, the pedestrian level is defined as 2 m [20,48], and a commonly used wind comfort criterion proposed by Murakami and Deguchi [74] (see Table 2) is adopted for the pedestrian wind comfort assessment. As presented in Table 2, Murakami and Deguchi suggested that an average wind speed of within 3 s could be regarded as the effective velocity U_e ; correspondingly, the pedestrian wind comfort quality could be categorized into four levels: classes A, B, C, and D. The result of the core area (1200 m \times 1200 m) of the campus is shown in Figure 21, in which the black boxes represent the building locations. It can be seen that in this wind scenario, there are three dangerous areas (i.e., The Eastern Football Stadium, Xinmin Road, and the lawn near The Old Gate) where wind can result in very serious effects on pedestrians. According the simulation results, the administrators can promptly remind students and staffs not to appear in the above areas if the campus suffers from a similar wind hazard.

Table 2. Wind comfort criterion proposed by Murakami and Deguchi [74].

Class	$U_e = \overline{U_{3s}}$	Wind Effects on Pedestrians
A	<5 m/s	No effect on people.
B	<10 m/s	Some effects on people.
C	<15 m/s	Serious effects on people.
D	≥ 15 m/s	Very serious effects on people.

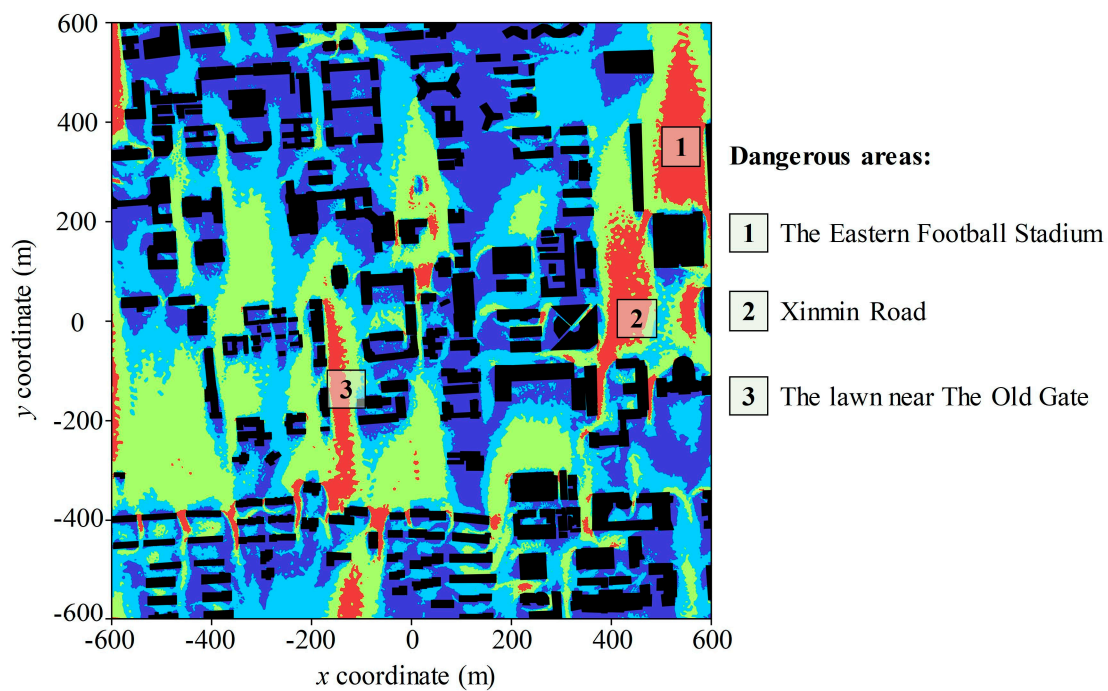


Figure 21. Visualization of the wind comfort quality class. Quality class A is in dark blue, class B in light blue, class C in yellow, and class D in red.

4.3. Multi-Hazard Simulation of the Office Building

4.3.1. Earthquake Simulation

The FE model of the four-story office building was generated on MSC.Marc software (Figure 22). The same El-Centro ground motion with $PGA = 0.4 g$ was inputted to the building along the x direction. Deformation at $t = 9$ s is displayed in Figure 23. The plastic hinges of the structure are mainly located at the bottom of the first-story column (Figure 24). The maximum inter-story drift ratio was 1.17%, representing a life-safe state according to the Chinese Code for Seismic Design of Buildings [71], which is compliant with the conclusions derived from the simulation of the entire campus.

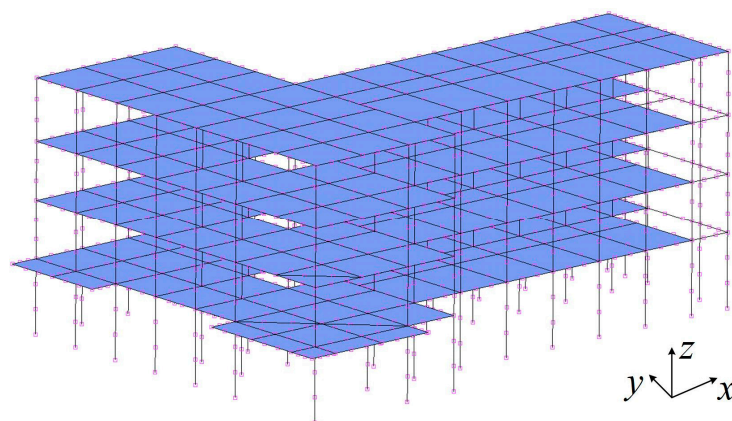


Figure 22. FE model of the office building.

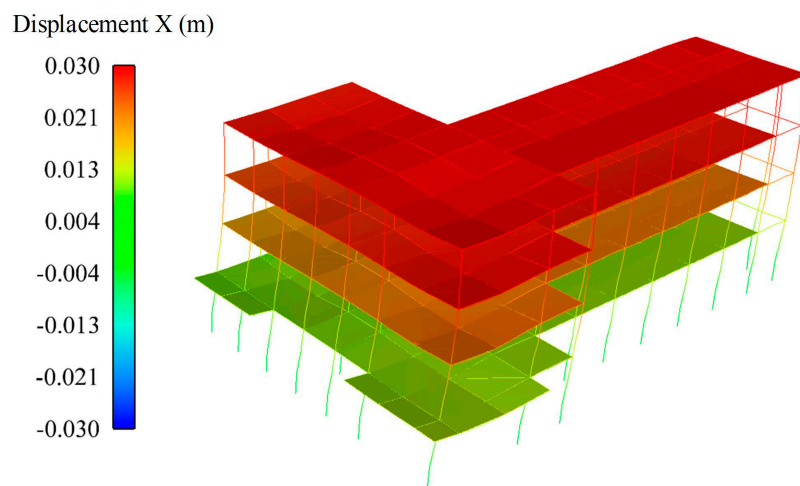


Figure 23. Deformation when $t = 9$ s.

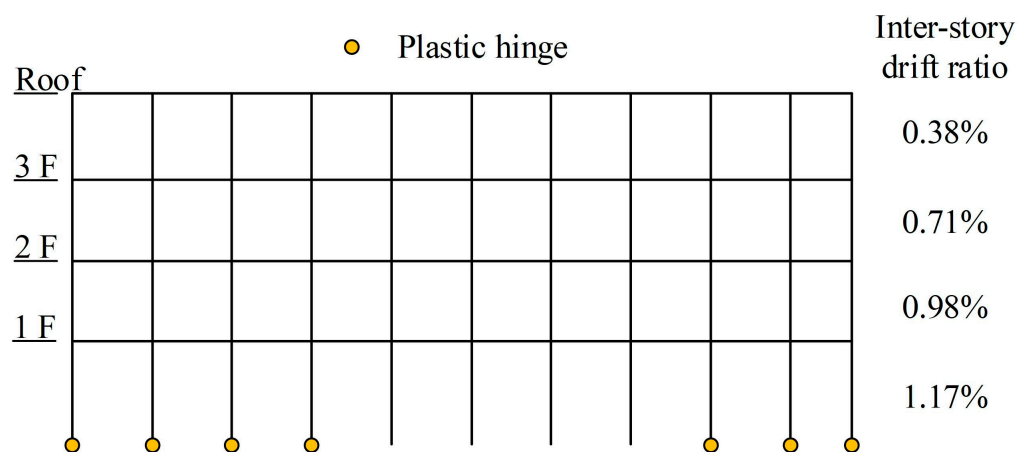


Figure 24. Plastic hinges and inter-story drift ratios of the office building.

4.3.2. Fire Simulation

For fire simulation, fire was assumed to have started in an office on the second story. The combustibles being ignited include a 1.5 m \times 0.2 m \times 0.2 m sofa cushion made of sponge and knitted fabric (Figure 25), undergoing polyurethane reactions [75]. The overall smoke distribution during fire development on the third story is illustrated in Figure 26. At $t = 300$ s, fire was fully developed, and the maximum temperature in the ignited office reached 470 °C. There are two evacuation stairways on the second story (Figure 25). According to the simulation, evacuation stair A is a better choice compared to evacuation stair B owing to its lower soot density during fire, as can be seen in Figure 26.

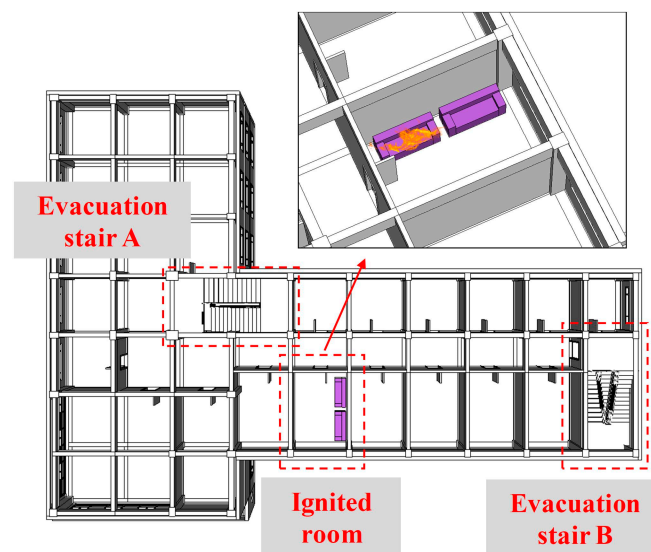


Figure 25. Details of the ignited room and evacuation stairs.

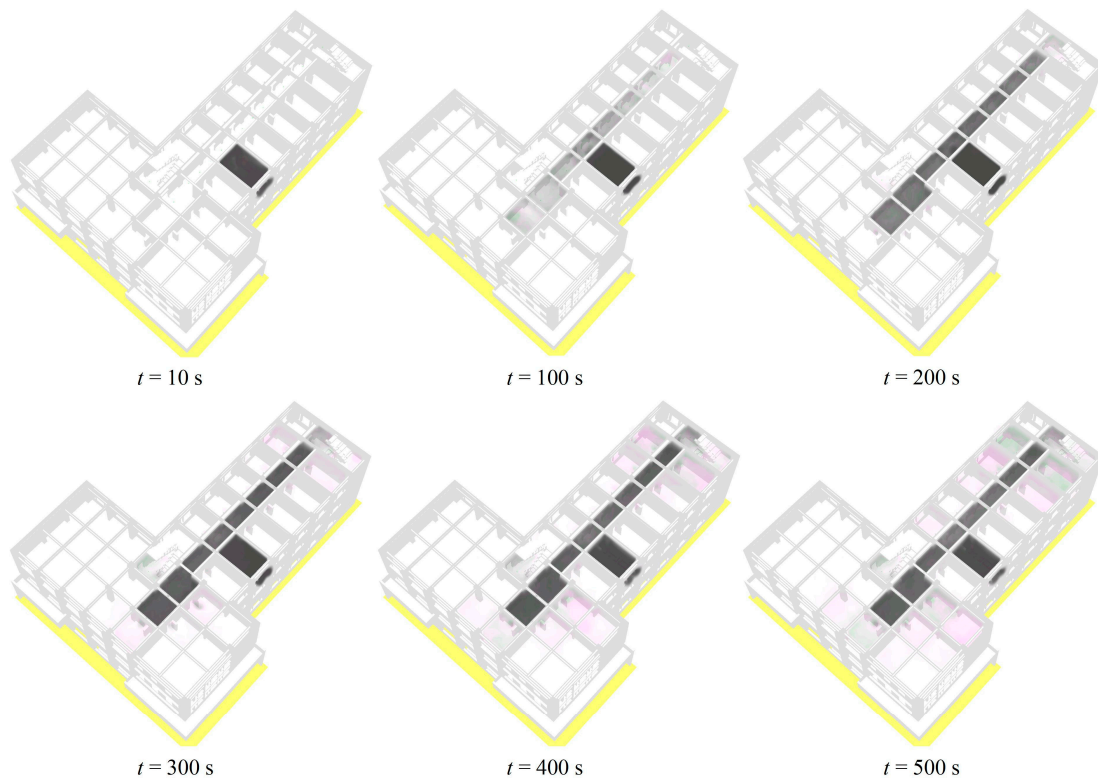


Figure 26. Time history of smoke distribution on the third story.

4.3.3. Wind Simulation

For wind simulation, as the office building is approximately $40.9 \text{ m} \times 29.8 \text{ m} \times 17.5 \text{ m}$, a computational domain of $394 \text{ m} \times 206 \text{ m} \times 106 \text{ m}$ was generated, ensuring an upstream length of $5 H$, downstream length of $15 H$, height of $6 H$, and distance of $5 H$ from the building to the lateral boundaries, which is in agreement with the COST 732 [62] and AIJ [63] best practice guidelines. Other simulation settings (turbulence model, boundary conditions, and equation solution method) were the same as those adopted in the case of the entire campus. As shown in Figure 27, the maximum positive and negative pressures on the exterior surfaces were approximately 389 Pa and -400 Pa ,

respectively, indicating that the office building is exposed to low risk in this scenario according to the fragility values specified in HAZUS, which is compliant with the conclusions derived from the simulation of the entire campus. It is worth noting that the information of the component on the building envelope (e.g., windows) can be easily extracted from the BIM, which greatly improves the efficiency of fragility analysis.

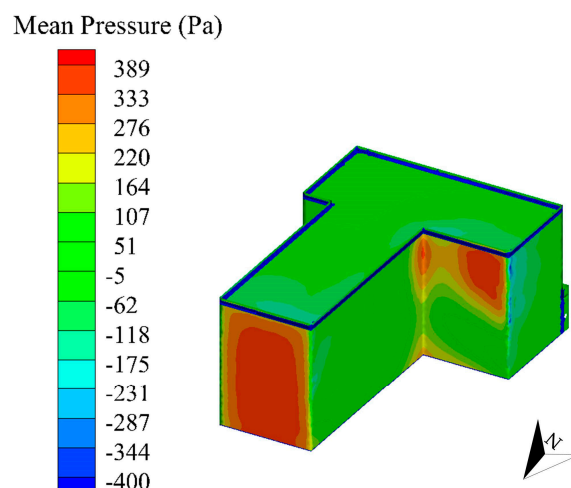


Figure 27. Wind pressure on the exterior surfaces of the building.

4.4. Brief Discussion

In the demonstrated cases, the global and detailed building data of the campus were integrated and unified in the CIM, based on which various hazard analyses of different types and scales were implemented. Consequently, powered by CIM, users have the freedom to choose different analysis modes and obtain simulation results at different scales, which cannot be realized through HAZUS or IN-CORE. Specifically, city-scale simulation results can be derived from the proposed simulation framework for urban areas, while the responses of detailed components can be derived from the proposed simulation framework for individual buildings, which meets the various demands of stakeholders. In addition, the CIM can be easily updated together with building construction and remodeling, which helps to establish a solid foundation for the risk assessment of regions and buildings.

Powered by the proposed multi-hazard simulation framework, the hazard resistance of the entire Tsinghua campus as well as its important buildings under specific earthquake, fire, and wind hazard conditions was assessed. The results show that the most severe threat to the entire Tsinghua campus is the earthquake hazard owing to its large number of unreinforced masonry structures. In contrast, fire and wind hazards are not severe problems. According to the simulated fire hazard scenario, only the fire resistance of the office buildings located in the southeast of the campus may need to be improved. According to the simulated wind hazard scenario, the non-structural components of the buildings in the campus are free from severe damage, and people should try not to appear in the three dangerous areas identified. In addition, the performance of the specific office building under multiple hazards is adequately good.

It should also be noted that all the analyses in this case study were based on physics-based models, which render the results convincing and thus offer administrators more confidence in decision making. Specifically, compared with the empirical or semi-empirical models adopted by HAZUS and IN-CORE, the city-scale nonlinear THA method for the earthquake simulation can rationally consider the specific features of the El-Centro ground motion and different types of buildings in the campus; the physics-based fire-spread model based on the thermal radiation and thermal plume mechanisms is capable of scientifically considering several important factors including the effects of weather conditions, fire resistance of buildings with different structural types, as well as different configurations

of building complexes; the CFD-based wind simulation method can reasonably consider the influence of adjacent buildings as well as the interaction between buildings and the terrain on the wind field of the campus. In addition, compared with the empirical or semi-empirical models that highly depend on historical disaster data, there is more room for improving the accuracy of physics-based models given the continuous increases in computing power. Furthermore, the high-fidelity visualizations of the simulation results can help the administrators of Tsinghua University in better understanding the hazard scenarios.

5. Conclusions

In this study, a CIM-powered multi-hazard simulation framework covering both individual buildings and urban areas considering earthquake, fire, and wind hazards was proposed. A case study of the Tsinghua University campus was undertaken to demonstrate the workflow of the proposed framework. The main conclusions of this study are as follows:

- (1) The database of the framework is a multi-scale model with CIM conception, which is capable of meeting the various demands of stakeholders. In addition, the unified data format can facilitate dynamic updates of building information in a built environment and promote the efficiency of multi-hazard simulations.
- (2) Hazard analyses in the proposed framework are all based on physics-based models, which lead to highly rational and accurate simulations. Compared with the empirical or semi-empirical models, there is more room for improving the accuracy of physics-based models due to continuously increasing computing power.
- (3) The proposed framework includes high-fidelity visualization of the results of the hazard analysis. Such visualization will help non-professional users in better understanding the hazard scenario, so that they can make their own contributions to hazard prevention and mitigation and thus encourage the use of multi-hazard simulation technology.

The proposed simulation framework can be utilized to obtain a favorable prediction of the resistances of both individual buildings and urban areas under multiple hazards, thus having great potential in helping stakeholders like city managers to assess and recognize the risks faced by the important buildings or the whole city more scientifically and efficiently. Based on this study, future research can be implemented on several topics such as the high-efficiency data architecture of the CIM platform, the deduction algorithms considering the coupling of multiple hazards, as well as the integration of all these data and algorithms, thereby realizing a truly integrated platform for multi-hazard simulations.

Author Contributions: Conceptualization, X.L. and D.G.; methodology, X.L. and D.G.; software, D.G.; validation, X.L. and D.G.; formal analysis, D.G.; investigation, D.G.; resources, X.L.; data curation, D.G.; writing—original draft preparation, D.G.; writing—review and editing, X.L., Z.X., C.X., and Y.T.; visualization, D.G.; supervision, X.L.; project administration, X.L.; funding acquisition, X.L. All authors have read and agreed to the published version of the manuscript.

Funding: This research was funded by the National Key R&D Program (grant number 2018YFC1504401) and the Tencent Foundation through the XPLOER PRIZE.

Acknowledgments: The authors would like to thank the Beijing Computing Center for providing the computational hardware and software that were used in this work.

Conflicts of Interest: The authors declare no conflicts of interest. The funders had no role in the design of the study; in the collection, analyses, or interpretation of data; in the writing of the manuscript, or in the decision to publish the results.

References

- Chen, X.S.; Liu, C.C.; Wu, I.C. A BIM-based visualization and warning system for fire rescue. *Adv. Eng. Inf.* **2018**, *37*, 42–53. [\[CrossRef\]](#)
- Lu, X.; Lu, X.Z.; Zhang, W.K.; Ye, L.P. Collapse simulation of a super high-rise building subjected to extremely strong earthquakes. *Sci. China-Techol. Sci.* **2011**, *54*, 2549–2560.
- Zheng, C.R.; Li, Y.S.; Wu, Y. Pedestrian-level wind environment on outdoor platforms of a thousand-meter-scale mega-tall building: Sub-configuration experiment and wind comfort assessment. *Build. Environ.* **2016**, *106*, 313–326. [\[CrossRef\]](#)
- Furukawa, A.; Ohta, Y. Failure process of masonry buildings during earthquake and associated casualty risk evaluation. *Nat. Hazards* **2009**, *49*, 25–51. [\[CrossRef\]](#)
- McKenna, F. OpenSees: A framework for earthquake engineering simulation. *Comput. Sci. Eng.* **2011**, *13*, 58–66. [\[CrossRef\]](#)
- Rehm, R.G.; Pitts, W.M.; Baum, H.R.; Evans, D.D.; Prasad, K.; McGrattan, K.B.; Forney, G.P. Initial model for fires in the World Trade Centre Towers. *Fire Saf. Sci. Proc. Int. Symp.* **2003**, *7*, 25–40. [\[CrossRef\]](#)
- Tominaga, Y.; Mochida, A.; Shirasawa, T.; Yoshie, R.; Kataoka, H.; Harimoto, K.; Nozu, T. Cross comparisons of CFD results of wind environment at pedestrian level around a high-rise building and within a building complex. *J. Asian Arch. Build. Eng.* **2004**, *3*, 63–70. [\[CrossRef\]](#)
- Xu, Z.; Zhang, Z.C.; Lu, X.Z.; Zeng, X.; Guan, H. Post-earthquake fire simulation considering overall seismic damage of sprinkler systems based on BIM and FEMA P-58. *Autom. Constr.* **2018**, *90*, 9–22. [\[CrossRef\]](#)
- HAZUS. Available online: <https://www.fema.gov/HAZUS> (accessed on 28 April 2019).
- Federal Emergency Management Agency (FEMA). *Multi-Hazard Loss Estimation Methodology-Earthquake Model, Hazus-MH2.1 Technical Manual*; FEMA: Washington, DC, USA, 2012.
- Hori, M. *Introduction to Computational Earthquake Engineering*; Imperial College Press: London, UK, 2006.
- Lu, X.Z.; Guan, H. *Earthquake Disaster Simulation of Civil Infrastructures: From Tall Buildings to Urban Areas*; Springer: Berlin/Heidelberg, Germany, 2017.
- Hamada, M. *Architectural Fire Resistant Themes*; Shokokusha: Tokyo, Japan, 1975.
- Himoto, K.; Tanaka, T. Development and validation of a physics-based urban fire spread model. *Fire Saf. J.* **2008**, *43*, 477–494. [\[CrossRef\]](#)
- Li, S.Z.; Davidson, R.A. Application of an urban fire simulation model. *Earthq. Spectra* **2013**, *29*, 1369–1389. [\[CrossRef\]](#)
- Rui, X.; Hui, S.; Yu, X.; Zhang, G.; Wu, B. Forest fire spread simulation algorithm based on cellular automata. *Nat. Hazards* **2018**, *91*, 309–319. [\[CrossRef\]](#)
- Zhao, S.J. GisFFE-an integrated software system for the dynamic simulation of fires following an earthquake based on GIS. *Fire Saf. J.* **2010**, *45*, 83–97. [\[CrossRef\]](#)
- Federal Emergency Management Agency (FEMA). *Multi-Hazard Loss Estimation Methodology-Hurricane Model, Hazus-MH2.1 Technical Manual*; FEMA: Washington, DC, USA, 2012.
- Chung, T.J. *Computational Fluid Dynamics*; Cambridge University Press: Cambridge, UK, 2010.
- Blocken, B.; Persoon, J. Pedestrian wind comfort around a large football stadium in an urban environment: CFD simulation, validation and application of the new Dutch wind nuisance standard. *J. Wind Eng. Ind. Aerodyn.* **2009**, *97*, 255–270. [\[CrossRef\]](#)
- Blocken, B.; Roels, S.; Carmeliet, J. Modification of pedestrian wind comfort in the Silvertop tower passages by an automatic control system. *J. Wind Eng. Ind. Aerodyn.* **2004**, *92*, 849–873. [\[CrossRef\]](#)
- Kang, G.; Kim, J.J.; Kim, D.J.; Choi, W.; Park, S.J. Development of a computational fluid dynamics model with tree drag parameterizations: Application to pedestrian wind comfort in an urban area. *Build. Environ.* **2017**, *124*, 209–218. [\[CrossRef\]](#)
- Leo, L.S.; Buccolieri, R.; Di Sabatino, S. Scale-adaptive morphometric analysis for urban air quality and ventilation applications. *Build. Res. Inf.* **2018**, *46*, 931–951. [\[CrossRef\]](#)
- Ng, E.; Yuan, C.; Chen, L.; Ren, C.; Fung, J.C. Improving the wind environment in high-density cities by understanding urban morphology and surface roughness: A study in Hong Kong. *Landsc. Urban Plan.* **2011**, *101*, 59–74. [\[CrossRef\]](#)

25. Song, J.; Fan, S.; Lin, W.; Mottet, L.; Woodward, H.; Davies Wykes, M.; Arcucci, R.; Xiao, D.; Debay, J.; ApSimon, H.; et al. Natural ventilation in cities: The implications of fluid mechanics. *Build. Res. Inf.* **2018**, *46*, 809–828. [\[CrossRef\]](#)
26. Vernay, D.G.; Raphael, B.; Smith, I.F. Augmenting simulations of airflow around buildings using field measurements. *Adv. Eng. Inf.* **2014**, *28*, 412–424. [\[CrossRef\]](#)
27. IN-CORE (Interdependent Networked Community Resilience Modelling Environment). Available online: http://resilience.colostate.edu/in_core.shtml (accessed on 24 April 2019).
28. Burrough, P.A.; McDonnell, R.A.; Lloyd, C.D. *Principles of Geographical Information Systems*; Oxford University Press: New York, USA, 2015.
29. Ding, L.Y.; Zhou, Y.; Akinci, B. Building Information Modelling (BIM) application framework: The process of expanding from 3D to computable nD. *Autom. Constr.* **2014**, *46*, 82–93. [\[CrossRef\]](#)
30. Xu, X.; Ding, L.Y.; Luo, H.B.; Ma, L. From building information modelling to city information modelling. *J. Inf. Technol. Constr.* **2014**, *19*, 292–307.
31. Schiefelbein, J.; Javadi, A.; Lauster, M.; Remmen, P.; Streblow, R.; Müller, D. Development of a city information model to support data management and analysis of building energy systems within complex city districts. In Proceedings of the International Conference CISBAT 2015 Future Buildings and Districts Sustainability from Nano to Urban Scale, Lausanne, Switzerland, 9–11 September 2015.
32. Padsala, R.; Coors, V. Conceptualizing, managing and developing: A web based 3D city information model for urban energy demand simulation. In Proceedings of the Eurographics Workshop on Urban Data Modelling and Visualisation, Delft, The Netherlands, 23 November 2015.
33. Monteiro, C.S.; Costa, C.; Pina, A.; Santos, M.Y.; Ferrão, P. An urban building database (UBD) supporting a smart city information system. *Energy Build.* **2018**, *158*, 244–260. [\[CrossRef\]](#)
34. Wang, H. Sensing information modelling for smart city. In Proceedings of the 2015 IEEE International Conference on Smart City/SocialCom/SustainCom (SmartCity), Chengdu, China, 15–17 December 2015.
35. Almeida, A.; Gonçalves, L.; Falcão, A.; Ildefonso, S. 3D-GIS heritage city model: Case study of the historical city of Leiria. In Proceedings of the 19th AGILE International Conference on Geographic Information Science, Helsinki, Finland, 14–17 June 2016.
36. Amirebrahimi, S.; Rajabifard, A.; Mendis, P.; Ngo, T. A framework for a microscale flood damage assessment and visualization for a building using BIM-GIS integration. *Int. J. Digit. Earth* **2016**, *9*, 363–386. [\[CrossRef\]](#)
37. Deng, Y.C.; Cheng, J.C.P.; Anumba, C. A framework for 3D traffic noise mapping using data from BIM and GIS integration. *Struct. Infrastruct. Eng.* **2016**, *12*, 1267–1280. [\[CrossRef\]](#)
38. De Laat, R.; Van Berlo, L. Integration of BIM and GIS: The development of the CityGML GeoBIM extension. In *3D Geo-Information Sciences*; Springer: Berlin/Heidelberg, Germany, 2011; pp. 211–225.
39. El-Mekawy, M.; Östman, A.; Shahzad, K. Towards interoperating CityGML and IFC building models: A unified model based approach. In *3D Geo-Information Sciences*; Springer: Berlin/Heidelberg, Germany, 2011; pp. 73–93.
40. Isikdag, U.; Underwood, J.; Aouad, G. An investigation into the applicability of building information models in geospatial environment in support of site selection and fire response management processes. *Adv. Eng. Inf.* **2008**, *22*, 504–519. [\[CrossRef\]](#)
41. Isikdag, U.; Zlatanova, S. Towards defining a framework for automatic generation of buildings in CityGML using building information models. In *3D Geo-Information Sciences*; Springer: Berlin/Heidelberg, Germany, 2009; pp. 79–96.
42. Niu, S.; Pan, W.; Zhao, Y. A BIM-GIS integrated web-based visualization system for low energy building design. *Procedia Eng.* **2015**, *121*, 2184–2192. [\[CrossRef\]](#)
43. Van Berlo, L. CityGML extension for building information modelling (BIM) and IFC. In Proceedings of the Free and Open Source Software for Geospatial (FOSS4G), Sydney, Australia, 1 July 2009.
44. Revit: Built for BIM. Available online: <http://www.autodesk.com/products/revit/overview> (accessed on 28 April 2019).
45. SuperMap GIS 9D (2019). Available online: <https://www.supermap.com/cn/2017/SuperMap-GIS-9D.asp> (accessed on 28 April 2019).
46. Lu, X.Z.; Zeng, X.; Xu, Z.; Guan, H. Physics-based simulation and high-fidelity visualization of fire following earthquake considering building seismic damage. *J. Earthqu. Eng.* **2019**, *23*, 1173–1193. [\[CrossRef\]](#)

47. Blocken, B.; Janssen, W.D.; Hooff, T. CFD simulation for pedestrian wind comfort and wind safety in urban areas: General decision framework and case study for the Eindhoven University campus. *Environ. Model. Softw.* **2012**, *30*, 15–34. [CrossRef]
48. Jacob, J.; Sagaut, P. Wind comfort assessment by means of large eddy simulation with lattice Boltzmann method in full scale city area. *Build. Environ.* **2018**, *139*, 110–124. [CrossRef]
49. Shi, X.; Zhu, Y.Y.; Duan, J.; Shao, R.Q.; Wang, J.G. Assessment of pedestrian wind environment in urban planning design. *Landsc. Urban Plan.* **2015**, *140*, 17–28. [CrossRef]
50. Hu, Z.Z.; Zhang, X.Y.; Wang, H.W.; Kassem, M. Improving interoperability between architectural and structural design models: An industry foundation classes-based approach with web-based tools. *Autom. Constr.* **2016**, *66*, 29–42. [CrossRef]
51. Oti, A.H.; Tizani, W.; Abanda, F.H.; Jaly-Zada, A.; Tah, J.H.M. Structural sustainability appraisal in BIM. *Autom. Constr.* **2016**, *69*, 44–58. [CrossRef]
52. Ramaji, I.J.; Memari, A.M. Interpretation of structural analytical models from the coordination view in building information models. *Autom. Constr.* **2018**, *90*, 117–133. [CrossRef]
53. Shin, T.S. Building information modelling (BIM) collaboration from the structural engineering perspective. *Int. J. Steel Struct.* **2017**, *17*, 205–214. [CrossRef]
54. Marc: Advanced Nonlinear Simulation Solution. Available online: <http://www.mscsoftware.com/product/marc> (accessed on 28 April 2019).
55. Zeng, X.; Lu, X.Z.; Xu, Z. Modelling technology for building aseismic elasto-plastic analysis based on BIM data. *Comput. Aided Eng.* **2014**, *23*, 5–11. (In Chinese)
56. Xu, Z.; Zhang, H.Z.; Lu, X.Z.; Xu, Y.J.; Zhang, Z.C.; Li, Y. A prediction method of building seismic loss based on BIM and FEMA P-58. *Autom. Constr.* **2019**, *90*, 245–257. [CrossRef]
57. Fire Dynamic Simulator (FDS) and Smokeview (SMV). Available online: <https://pages.nist.gov/fds-smv> (accessed on 28 April 2019).
58. Pyrosim. Available online: <https://www.thunderheadeng.com/pyrosim> (accessed on 28 April 2019).
59. Xu, Z.; Lu, X.Z.; Guan, H.; Chen, C.; Ren, A.Z. A virtual reality based fire training simulator with smoke hazard assessment capacity. *Adv. Eng. Softw.* **2014**, *68*, 1–8. [CrossRef]
60. Fluent. Available online: <https://www.ansys.com/products/fluids/ansys-fluent> (accessed on 28 April 2019).
61. Dynamo BIM. Available online: <http://dynamobim.org> (accessed on 28 April 2019).
62. Franke, J.; Hellsten, A.; Schlünzen, H.; Carissimo, B. *Best Practice Guideline for the CFD Simulation of Flows in the Urban Environment, Cost Action 732: Quality Assurance and Improvement of Microscale Meteorological Models*; COST Office: Brussels, Belgium, 2007.
63. Tominaga, Y.; Mochida, A.; Yoshie, R.; Kataoka, H.; Nozu, T.; Yoshikawa, M.; Shirasawa, T. AIJ guidelines for practical applications of CFD to pedestrian wind environment around buildings. *J. Wind Eng. Ind. Aerodyn.* **2008**, *96*, 1749–1761. [CrossRef]
64. Tecplot 360. Available online: <https://www.tecplot.com/products/tecplot-360> (accessed on 28 April 2019).
65. OpenSceneGraph. Available online: <http://www.openscenegraph.org> (accessed on 28 April 2019).
66. Xiong, C.; Lu, X.Z.; Hori, M.; Guan, H.; Xu, Z. Building seismic response and visualization using 3D urban polygonal modelling. *Autom. Constr.* **2015**, *55*, 25–34. [CrossRef]
67. Xiong, C.; Lu, X.Z.; Huang, J.; Guan, H. Multi-LOD seismic-damage simulation of urban buildings and case study in Beijing CBD. *Bull. Earthq. Eng.* **2019**, *17*, 2037–2057. [CrossRef]
68. Zeng, X.; Lu, X.Z.; Yang, T.; Xu, Z. Application of the FEMA-P58 methodology for regional earthquake loss prediction. *Nat. Hazards* **2016**, *83*, 177–192. [CrossRef]
69. Mechanical Pro. Available online: <https://www.ansys.com/products/structures/ansys-mechanical-pro> (accessed on 28 April 2019).
70. Iqbal, Q.M.Z.; Chan, A.L.S. Pedestrian level wind environment assessment around group of high-rise cross-shaped buildings: Effect of building shape, separation and orientation. *Build. Environ.* **2016**, *101*, 45–63. [CrossRef] [PubMed]
71. Ministry of Housing and Urban-Rural Development of the People's Republic of China (MOHURD). *Code for Seismic Design of Buildings, GB50011-2010*; China Architecture Industry Press: Beijing, China, 2010. (In Chinese)
72. Xiong, C.; Lu, X.Z.; Lin, X.C.; Xu, Z.; Ye, L.P. Parameter determination and damage assessment for THA-based regional seismic damage prediction of multi-story buildings. *J. Earthqu. Eng.* **2017**, *21*, 461–485. [CrossRef]

73. Ministry of Housing and Urban-Rural Development of the People's Republic of China (MOHURD). *Load Code for the Design of Building Structures, GB50009-2012*; China Architecture Industry Press: Beijing, China, 2012. (In Chinese)
74. Murakami, S.; Deguchi, K. New criteria for wind effects on pedestrians. *J. Wind Eng. Ind. Aerodyn.* **1981**, *7*, 289–309. [[CrossRef](#)]
75. McGrattan, K.; Hostikka, S.; McDermott, R.; Floyd, J.; Weinschenk, C.; Overholt, K. *Fire Dynamics Simulator User's Guide*, 6th ed.; U.S. Department of Commerce, National Institute of Standards and Technology (NIST): Gaithersburg, MD, USA, 2017.



© 2020 by the authors. Licensee MDPI, Basel, Switzerland. This article is an open access article distributed under the terms and conditions of the Creative Commons Attribution (CC BY) license (<http://creativecommons.org/licenses/by/4.0/>).